Rail to Digital automated up to autonomous train operation

D48.5 – Test planning execution and analysis of Short Range Communications (SRC) and Relative Localisation (RL)

Due date of deliverable: 31/05/2026

Actual submission date: 28/02/2026

Leader/Responsible of this Deliverable: Paul Unterhuber, DLR

Reviewed: Y

Document status		
Revision	Date	Description
01	26/06/2025	First issue
02	01/08/2025	Chapter 3, 4 and 5 drafted
03	23/12/2025	Chapter 6 and 7 drafted
04	30/01/2026	Final Document for TMT review
05	12/03/2026	TMT and SteCo review included
06	19/06/2026	EU-Rail JU review included

Project funded from the European Union's Horizon Europe research and innovation programme		
Dissemination Level		
PU	Public	x
SEN	Sensitiv – limited under the conditions of the Grant Agreement	

Start date: 01/12/2022 Duration: 42 months

ACKNOWLEDGEMENTS

This project has received funding from the Europe's Rail Joint Undertaking (ERJU) under the Grant Agreement no. 101102001. The JU receives support from the European Union's Horizon Europe research and innovation programme and the Europe's Rail JU members other than the Union.

REPORT CONTRIBUTORS

Name	Company	Details of Contribution
Paul Unterhuber	DLR	All
Jeroen Braakman	NS	Review
Andreas Lehner	DLR	Review
Kevin Mullankuzhy	DLR	Contribution to Chapter 7

EXECUTIVE SUMMARY

This deliverable presents the results of a comprehensive testing campaign conducted under Work Package 48 (WP48) of the FP2R2DATO project, focusing on the validation of Short-Range Communication (SRC) and Relative Localization (RL) as core enablers for high-automation rail operations, including Virtually Coupled Train Sets (VCTS) and Self-Driving Freight Wagons (SDFW).

The tests were carried out with Nederlandse Spoorwegen (NS) in a representative railway environment characterized by overhead lines, multiple parallel tracks, parked trains, and surrounding infrastructure in Amersfoort, Netherlands. This setting provided a realistic and challenging testbed for evaluating the performance of Train-to-Train (T2T) communication and localization under real-world conditions.

The evaluation was based on a Ultra-Wideband (UWB) test system developed by the German Aerospace Center (DLR), utilizing IEEE 802.15.4 chipsets. Two antenna configurations (omni-directional and directional) were tested in parallel. Results show that SRC achieved reliable data exchange with minimal packet loss, even at distances up to 250 meters. Directional antennas demonstrated superior performance due to reduced interference, but reliable communication was also achieved with omni-directional setups, which confirms the technology's robustness across different configurations.

For RL, the tests achieved a distance estimation accuracy of ±20 cm to ±80 cm across the full operational range. This level of precision unmatched by most alternative technologies in complex rail environments is critical for safe gap supervision, dynamic spacing control, and collision avoidance in virtual coupling scenarios.

Together, the results demonstrate that the selected T2T-based SRC and RL system delivers the communication and distance performance required for safety-critical functions in autonomous rail operations. The technology enables decentralized, real-time coordination between rail vehicles, enhancing system resilience, operational flexibility, and safety.

The findings confirm that SRC and RL are not only technically viable but also well-suited for integration into future VCTS onboard architectures, supporting advanced control and supervision concepts while reducing dependency on fixed infrastructure.

While this deliverable establishes a strong foundation, further research is needed to explore the impact of these technologies on intra-platoon dynamics, control stability, and system-level safety under diverse operational conditions. The results provide a clear roadmap for future projects.

In summary, this testing campaign clearly showed the capabilities of T2T communication in real rail environments and the potential of the combination of communication and distance estimation.

ABBREVIATIONS AND ACRONYMS

3GPP	3rd Generation Partnership Project
4G	Fourth Generation
AnRS	Autonomous Route Setting
ASTP	Absolute Safe Train Positioning
ATO	Automatic Train Operation
DS-RTT	Double Sided Round Trip Time
ETRS89	European Terrestrial Reference System 1989
FRMCS	Future Railway Mobile Communication System
GNSS	Global Navigation Satellite System
IEEE	Institute of Electrical and Electronics Engineers
JU	Junt Undertaking
LAN	Local Area Network
LiDAR	Light Detection and Ranging
LTE	Long Term Evolution
LoS	Line of Sight
MPC	Multipath Components
NTP	Network Time Protocol
PD	Power Delivery
PER	Packet Error Rate
R2DATO	Rail to Digital automated up to autonomous train operation
RL	Relative Localization
RMSE	Root Mean Square Error
ROS	Robot Operating System
RTK	Real-Time Kinematic
RTT	Round Trip Time
SBF	Sepentrio Binary Format
SDFW	Self Driving Freight Wagon
SNR	Signal to Noise Ratio
SRC	Short Range Communication
T2T	Train-to-Train
USB	Universal Serial Bus

UTM	Universal Transverse Mercator
UWB	Ultra Wide Band
VCTS	Virtually Coupled Train Sets
VPN	Virtual Private Network
WGS84	World Geodetic System 1984
WLAN	Wireless LAN
WP	Work Package

TABLE OF CONTENTS

LIST OF FIGURES

LIST OF TABLES

2 INTRODUCTION

Work Package 48 (WP48) of the FP2R2DATO project is dedicated to advancing the technological foundations for high-automation and near-autonomous rail operations, with a particular focus on enabling Virtually Coupled Train Sets (VCTS) and Self-Driving Freight Wagons (SDFW). These innovative operational concepts represent a paradigm shift from traditional, mechanically coupled train formations toward decentralized, intelligent, and dynamically coordinated rail systems. The success of such systems critically depends on the availability of reliable, low-latency short range communication (SRC) and high-precision relative localization (RL) between rail vehicles. These capabilities are not adequately addressed by existing communication systems or absolute positioning solutions alone.
To bridge this gap, WP48 has identified SRC and RL as two pivotal technologies developed under Task 48.4. SRC establishes a direct, high-performance wireless link between moving rail vehicles. This technology is designed to support real-time, bidirectional data exchange and resilience to multipath fading, interference, and rapid topology changes due to vehicle movement. Unlike broader communication systems such as the Future Railway Mobile Communication System (FRMCS), which is optimized for wide-area coverage and infrastructure-based connectivity, SRC operates at the train-to-train (T2T) level, enabling immediate, decentralized decision-making and control.

Based on SRC, RL provides a high-accuracy estimation of the distance and relative position between two communication nodes based on time-of-flight measurements. RL is not intended to replace Advanced Safe Train Positioning (ASTP), which provides globally referenced, safety-certified location data (covered in WP21 and WP22), but rather to augment it with fine-grained, dynamic relative localization. This is essential for maintaining control stability in VCTS, where the distance between units must be maintained within centimeter-level tolerances during acceleration, braking, and curve negotiation. Furthermore, SRC and RL is a key enabler for collision avoidance for innovative operational solutions, where trains or wagons must react instantly to proximity events without relying on infrastructure-based detection.
The integration of SRC and RL is therefore not merely additive, it is synergistic and mission-critical. Only when both technologies operate in concert can the safety, performance, and operational flexibility required for railway operation with headways relative to braking capabilities be achieved. A state-of-the-art analysis, the theoretical backgrounds and the development of the SRC and RL test system was documented in FP2R2DATO D48.4.

To validate the performance and robustness of SRC and RL system based on ultra-wide-band communication under realistic rail conditions, a comprehensive field testing campaign was conducted in Amersfoort, Netherlands. The testing was designed to simulate a wide range of operational scenarios, including:

- VCTS coupling and de-coupling
- Approaching parked rail vehicles like SDFW
- Driving two trains in short distance like a VCTS
- Environment sensing for collision avoidance

Each test scenario was instrumented with high-precision reference systems including Real-Time Kinematic positioning (RTK)-GNSS, laser trackers, and inertial measurement units (IMUs) to provide ground-truth data for validating both SRC performance and RL accuracy.

The deliverable is structured as follows: In Chapter 3 the architecture and installed test equipment, the reference systems and sensors are described in detail. The test preparation including pre-tests, scenarios, schedules and safety is addressed in Chapter 4.
The test report is documented in detail in Chapter 5: Achievements for each test case and in public relations, provide a complete record of data acquisition protocols, and lessons learned.
Chapter 6 provides all details about the Analysis of Test Data.

Finally, Chapter 7 synthesizes the findings, underscores the maturity of SRC and RL as viable technologies for deployment in future autonomous rail systems, and outlines a clear path forward. It identifies key areas for further research and recommends follow-up activities for future in upcoming projects.

3 TEST EQUIPMENT

For the purpose of SRC and RL tests in a railway environment an UWB communication system was developed. The test equipment was installed on a regional train of NS (Sprinter New Generation class), with equipment being placed on the coupler and inside of the train cabin. As one train was also used for ATO testing, this train is called **Train ATO**, the other train is called **Train X** in the following sections. The development of the test equipment, the supporting equipment and a ground truth system was reported in FP2R2DATO D48.4. The resulting architecture and the final installation, as well of a description of each component is summarized in this chapter.

3.1 ARCHITECTURE AND INSTALLATION

The architecture of the test setup shown in Figure 1 can be split in six major nodes:

- Node A: First T2T communication unit and located on the **Train ATO**.
  - 1 UWB double chip unit
  - 1 LTE uplink and network switch
  - 1 GNSS
  - 2 Sensors
  - 1 Lidar
  - 4 Raspberry Pis 4B
  - Power
- Node B: Second T2T communication unit called **Train X** mounted either on the second train or on a tripod in front a buffer stop.
  - 1 UWB double chip unit
  - 1 LTE uplink and network switch
  - 1 GNSS
  - 1 Raspberry Pis 4B
  - Power
- Node C: The third communication unit was used as static **Ground** station.
  - 1 UWB double chip unit
  - 1 LTE uplink and network switch
  - 1 GNSS
  - 1 Raspberry Pis 4B
  - Power
- Node D: For sensing applications and obstacle detection this unit was used as **Track worker**.
  - 1 UWB single chip unit
  - 1 Raspberry Pis 4B
  - Power
- Node E: For controlling the test units and status recording this node was set as **Controller**.
  - 1 Laptop

- 1 LTE uplink
- Node F: A **Leica** Total Station was used as position reference system.
  - 1 Leica Total Station
  - 1 Laptop

The architecture, implementation and setup of all nodes was performed by DLR. All nodes have been installed in stand-alone boxes that are easy to handle and can be mounted on the trains if required. Furthermore, each node was self-powered and equipped with an LTE modem or network connection for remote access. The nodes are explained in more detail in the next sections.

3.2 Ultra-Wideband Communication

The core of the test equipment were the ultra-wideband communication nodes with different antenna settings. Technical details can be found in FP2R2DATO D48.4.

3.2.1 Nodes

Four UWB nodes were used in three different settings. For Train ATO shown in Figure 2 and Train X shown in Figure 3 the nodes were equipped with two Qorvo DW1000 chips, set in active mode on two different UWB channels (two and five) and connected to two different external antennas (omni-directional and directional). In active mode, the nodes were transmitting and receiving data packets; one node was set as leader, all others as followers.

The Ground node was based on two Qorvo DW1000 chips, both set in passive mode. As passive node, the Ground only received the data traffic between the nodes from Train ATO, Train X and in one case from the Track worker. The Ground node was equipped with two external omni-directional antennas spaced in two lambda distance. The frequency selection was varied between both chips, operating at channel two on one chip and on channel five on the other chip. Details can be found in Table 1.

For future joint communication and sensing (JCAS) applications test scenarios with Track workers were simulated. One or multiple persons without communication nodes were crossing the railway track in safe distance to the Train ATO which was driving back and forth. For one test, one person was equipped with a communication node based on a single Qorvo DW1000 chip and omni-directional chip antenna. The node was set at channel 2 in active mode. The Track worker was walking along the railway track and crossing the rails while the Train ATO was standing.

3.2.2 Antennas

Three different antennas were used for the UWB tests. The goal was to evaluate the difference of omni-directional and directional antennas. Dependent on the final application, a recommendation can be given for the one or the other type. In the Train ATO and Train X nodes an omni-directional and a directional antenna was installed. The estimated phase centers of both antennas were placed on top each other. For GNSS reception, one antenna was installed on top of the boxes as well. Details can be seen in Figure 2.

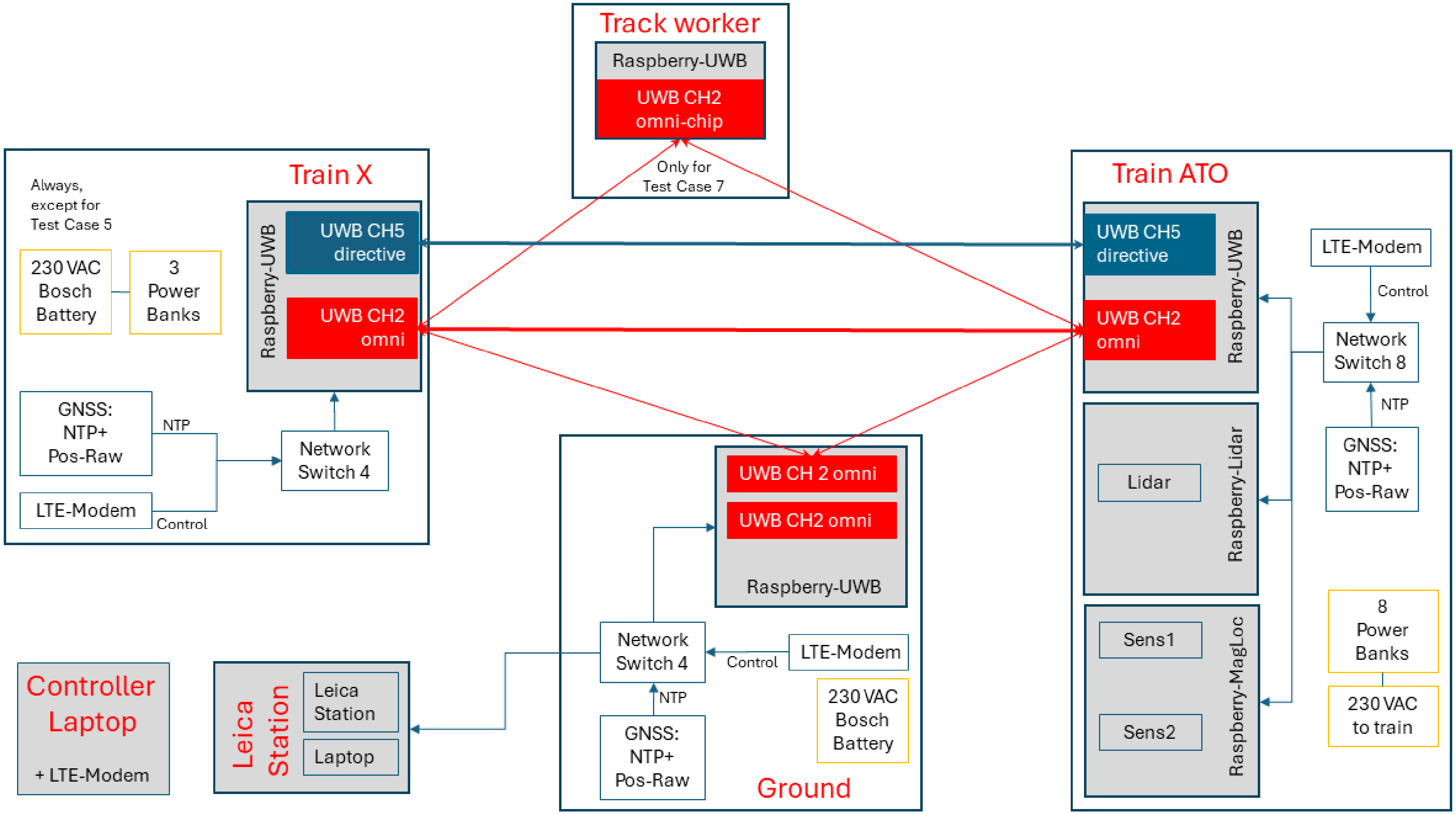

Figure 1: Test equipment architecture

3.2.2.1 Omni-directional antenna

In an ideal case, omni-directional antennas offer a uniform distribution of the antenna gain in all directions. Dipole or monopole antennas offer a donut shape antenna gain which reflects a more or less uniform distribution in the azimuth plane. Hence, the transmission and reception of signals experience a similar gain in this one plane. We use the Taoglas TU.60.3H31 Wideband Dipole with N connector. This antenna is designed for 3.5-8 GHz with a gain of 1.9 dBi at 4 GHz [1].

3.2.2.2 Directional antenna

Directional antennas focus the gain in one dedicated direction indicated with the opening angle or 3 dB beam width. Dependent on the opening angle, amplification is available in the main lobe. We used the Taoglas PHA.01.A UWB antenna with a size of 200x150x252 mm and an external N connector. This horn antenna offers a gain of 16 dBi and 17 dBi in the frequency ranges of 3.7 GHz to 4.2 GHz and 6.25 GHz to 6.75 GHz, respectively. The main lobe has an opening angle of 17° [2].

3.2.2.3 Omni-directional chip antenna

The Partron Dielectric Chip Antenna UWB8B with the part number ACS5200HFAUWB was used for the trackworker UWB device. The antenna offers a more or less omni-directional antenna pattern in the azimuth plane for a frequency range from 3.2 GHz to 7.2 GHz [3].

3.3 SENSORS

Two Inertial Measurement Units (IMUs) MTi-610 from XSens were used in node A to collect the magnetic field, the force and turn rates of the train. Each sensor was connected to a Raspberry Pi 4B for controlling and data storage. Two sensors were mounted in same orientation on the front and back plane of the case.

3.3.1.1 Magnetometer

The magnetometers measure the three components of the magnetic field. Magnetic measurements can be used as a complement to radio ranging as they allow for absolute along-track localization [4], [5] as well as for relative localization for distances greater than the range of UWB ranging even in situations of GNSS degradation or unavailability [6]. Additionally, it is possible to identify the track on which the train is located with magnetic field measurements [7]. Conversely, radio communication and ranging between trains equipped with magnetometers for localization can be used to enhance the reliability and the performance of the magnetic field-based absolute localization.

3.3.1.2 Accelerometers and gyroscopes

Accelerometers and gyroscopes measure the acceleration respectively the turn rates. An overview of the accelerometers and gyroscope measurements mounted on trains is provided in [8]. In particular, accelerometers and gyroscopes can be used as a standalone solution for positioning along short distances using dead-reckoning or as a part of a sensor fusion solution combined with absolute positioning solutions such as GNSS or magnetic field-based localization [9], [10]. It has also been shown that fusing UWB measurements with accelerometer and gyroscope measurements can enhance accuracy and robustness [11].

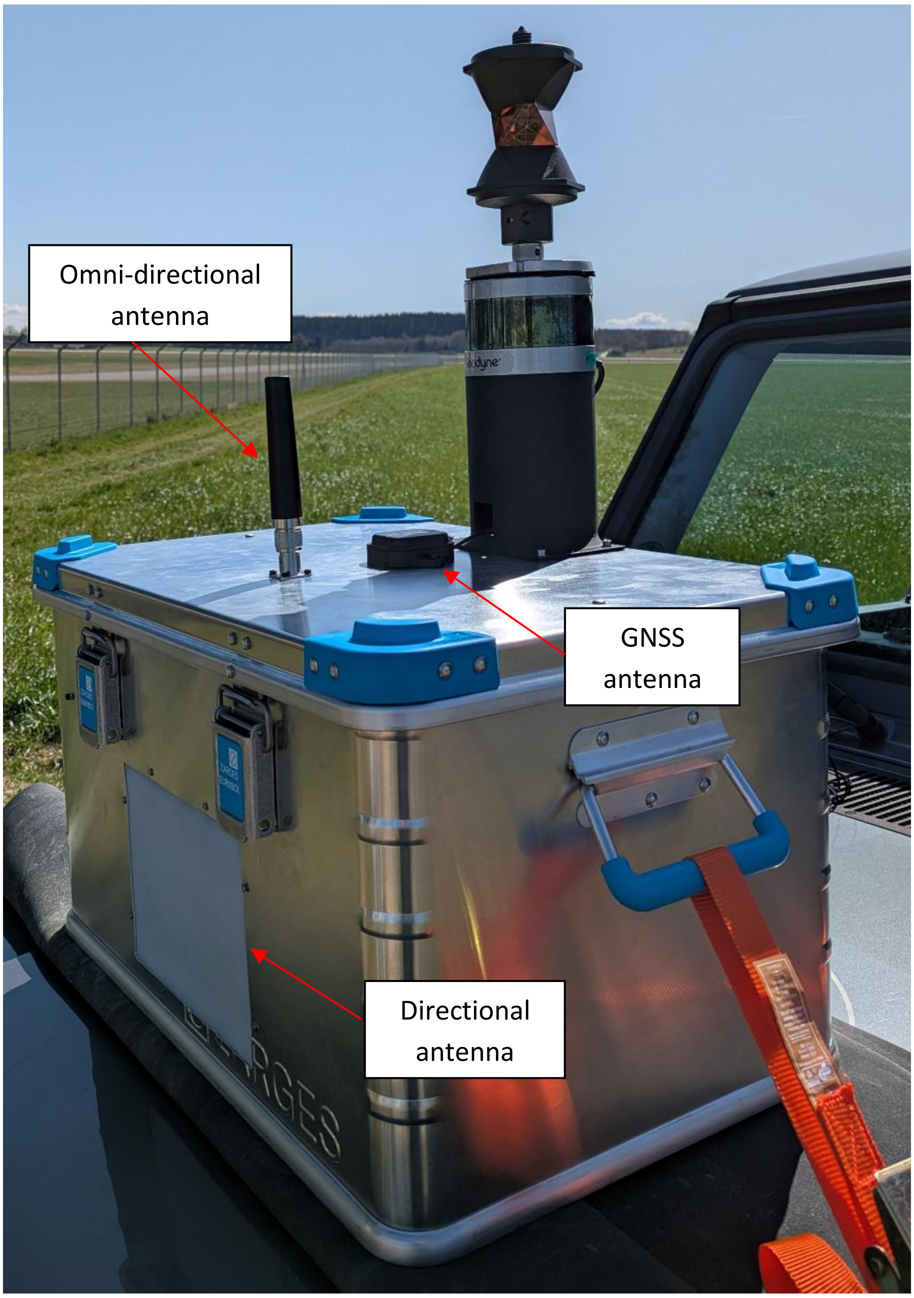

Figure 2: Hardware setup and equipment integration for Train ATO

3.4 Timing System and Absolute Positionig

In the three main nodes Septentrio PolaRx 5 Global Navigation Satellite System (GNSS) receivers were installed. At Train ATO and Train X uBlox ANN-MB-00-00 GNSS antennas were used as shown in Figure 2. At the Ground node, a Septentrio PolaNt-x MF GNSS antenna was installed. All used GNSS antennas were able to receive multi-constellation and multi-frequency signals. The use of the GNSS in each node was covering two requirements.

First, all nodes should be synchronized by a common time. Hence, all used GNSS receivers were set up as Network Time Protocol (NTP) server and spread the common GNSS time via the Local

Area Network (LAN) to all subsystems in each node. This ensures all recorded data stamped on the same time base and facilitate the post processing.

Second, the GNSS receivers recorded the received raw data for absolute positioning of the Node A, B and C. In post processing the position and the movement of Train ATO, Train X and the Ground station can be evaluated. A detailed analysis of the influence of the railway environment on the GNSS based position accuracy can be performed. The train body itself, close other trains, overhead line system, buildings and trees may cause multipath components (MPCs) or shadowing which degrades the accuracy of the position estimate. The GNSS position can be compared against the ground truth system position estimation.

3.5 GROUND TRUTH

For evaluating the position and relative localization data, a ground truth system was installed. Based on the test scenarios, the ground truth is covering the absolute position of one moving train with the Leica, or the relative distance between two moving trains with the LiDAR.

3.5.1 Leica

The Leica Total Station (TS) MS60 is positioned next to the railway tracks and leveled to several fixed points in the close surrounding. Based on the fixed points, the TS can be moved to different locations but remains in the same coordinate system. The emitted laser signal is reflected by the prism reflector and collected by the TS again. The prism is mounted on the unit to be measured or tracked as shown in Figure 4.

The TS was used in tracking mode and the collected data was streamed to a laptop. The laptop stored the TS data with a time stamp provided by the GNSS NTP server. Therefore, the Leica-Laptop was connected via cable with the GNSS receiver of the Ground station as shown in Figure 1.

3.5.2 LiDAR

A Velodyne Puck VLP-16 Light Detection and Ranging (LiDAR) device was mounted on the Train ATO as shown in Figure 5. The LiDAR scans on 16 planes the 360° surrounding up to 100 m distance. A Raspberry Pi 4B is used as controller and for data storage of the collected point cloud. As the LiDAR is mounted right in front of the train, the visual field of the LiDAR was reduced to ±105°. The main objective of the LiDAR is to provide a ground truth for the VCTS test scenarios. In these scenarios the Train ATO and the Train X are driving in short distance on the same track. As the Leica TS is only capable to track the Train ATO, the LiDAR records the Train X driving in front of the Train ATO. Based on the recorded point cloud, the distance between the two trains is estimated and used as ground truth.

For a detailed analysis of the environment, the LiDAR point cloud could be used as well. Parked trains, the overhead system or installed equipment is visible in the point cloud. In combination with the absolute position of the Train ATO provided by the Leica measurements, a very accurate model of the environment can be provided.

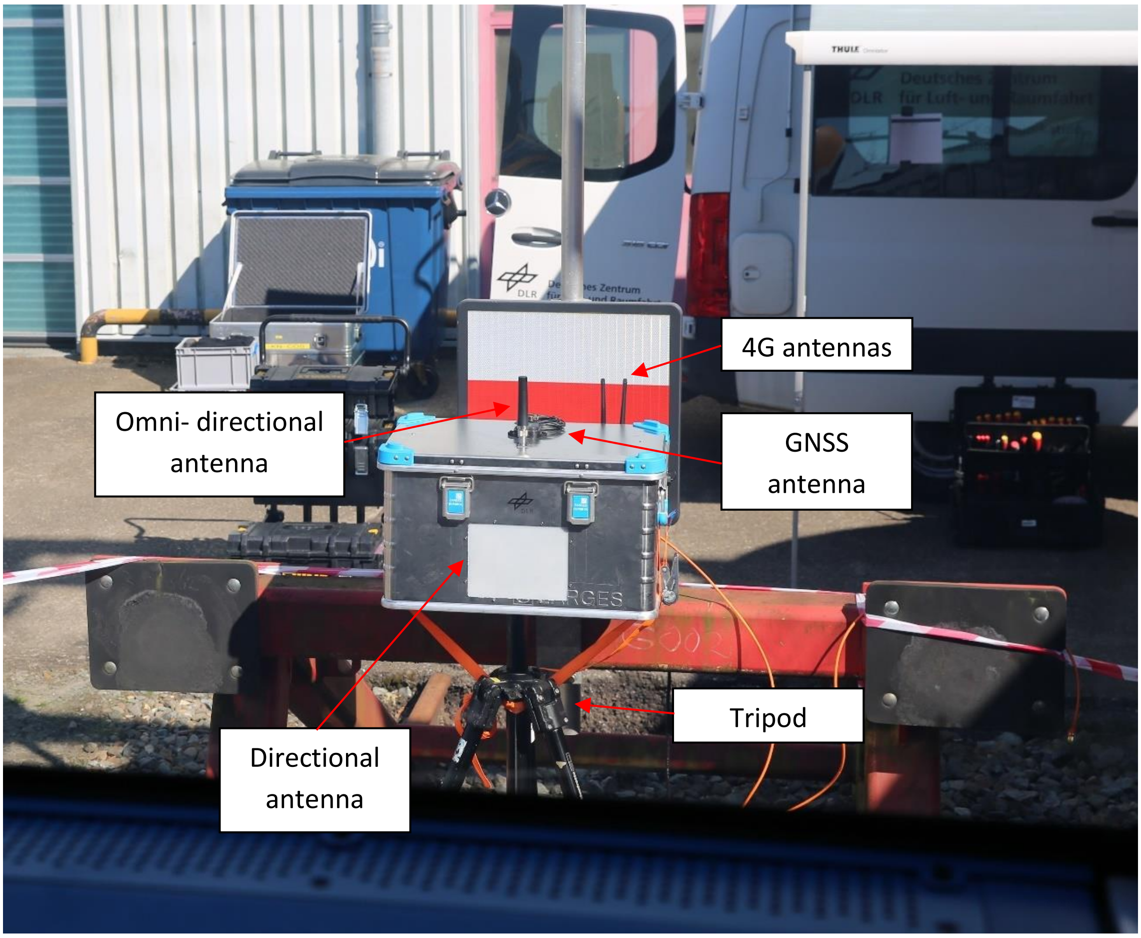

Figure 3: Hardware setup Train X

3.6 Control

In all test scenarios, the nodes were located up to 350 m apart from each other and/or moving with the trains. Hence, a wireless based control network was necessary to start and stop the recording of the test data, to observe the status during tests, and to provide real time results for the VCTS show case. Due to the large area and the difficult propagation scenarios in the shunting yard, a public cellular communication system was preferred against a wireless LAN (WLAN) based system.

The used Teltonika RUT241 modems are supporting 3rd Generation Partnership Project (3GPP) release 10 which support 4G Long Term Evolution (LTE) Cat 4 communication. Based on the public 4G network a Virtual Private Network (VPN) was established with WireGuard. This setup allowed a secure remote access to all Raspberry Pis in the Nodes Train ATO, Train X, Ground from the Controller laptop and from back-office support at DLR Institute of Communications and Navigation, Oberpfaffenhofen, Germany. The real time data acquisition and demonstration of the RL distance estimation on the Controller laptop was also performed via the control network as shown in Figure 6.

3.7 POWER

Due to the position of installation in front of the train on the coupler, or next to the railway track several hundred meters away from the next power socket, all nodes were designed to work standalone without external powering. Based on power banks supporting Universal Serial Bus (USB) 3.1 Typ-C Power Delivery (PD) the components inside each node could be supplied with 5 V, 9V, 12 V or 15 V up to 140 Watt. Each device was powered by one Intenso HE25000 power bank. These power banks support simultaneous charging and discharging without a drop in the PD output power when the state changes. For the case if external 230 VAC power was available, all power banks were connected to 230 VAC to USB-C power adapters. The power banks and the power adapters were mounted inside the box. Only a common 230 VAC connection was routed to the outside.

Temporarily charging was possible at the Train ATO with a 230 VAC provided by the train itself, at the Train X either by the used train itself, or provided by a Bosch GEN 230-1500 battery when the Train X was static positioned in front of the buffer stop without a train.

The Ground station was powered directly by a Bosch GEN 230-1500 battery. The Leica TS including the laptop, the Controller laptop and cameras were running on internal batteries and charged at the DLR's measurement van. The van provides 230 VAC by internal batteries 12 VDC and inverters.

Figure 4: Ground truth Leica TS MS60

Figure 5: Ground truth LiDAR Velodyne Puck VLP-16

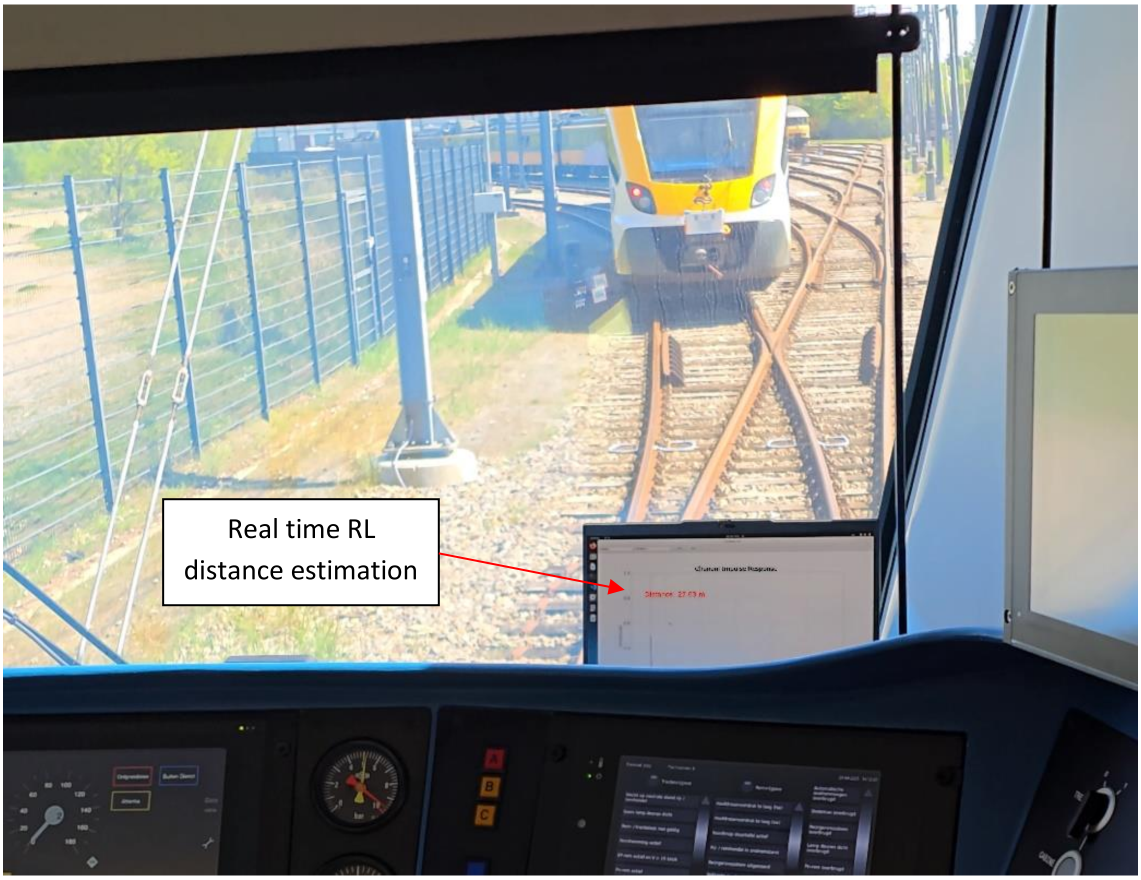

Figure 6: Controller Laptop for VCTS show case via 4G control network

4 TEST PREPARATION

The test preparation encompasses the hardware development and pre-tests, the test scenarios, the test schedule and the safety instructions. The majority of the preparation was performed by DLR in close exchange with NS. NS focused on the organization and availability of trains, tracks, train drivers and safety guards. Furthermore, a risk assessment of the tests was performed.

4.1 Hardware Development and Pre-tests

The hardware for the tests was developed in five steps:

1. Development of UWB test equipment: As described in detail in FP2R2DATO D48.4 Chapter 6, the UWB nodes are an inhouse development of DLR based on Qorvo DW1000 chip sets. In particular, the implementation with two synchronized chips on one board, the peripheral of the chips, the firmware and test data acquisition software were developed.
2. Lab test inside: Lab tests were conducted either with cables and attenuators, or with antennas in short distance between the nodes in DLR laboratories. The hardware and firmware were analyzed, adapted and improved for the target application.
3. On-site inspection of test environment and trains: Representatives of DLR and NS inspected the shunting yard environment in Amersfoort. The implementation and the mounting on the train of the test equipment was discussed, the scale of the tests was agreed and the limitations of the maneuvers were clarified.
4. Lab test outside: The different antenna settings and the desired communication range was tested. The antenna setting of the Train ATO and Train X with one omni-directional and one directional antenna was fixed. After the lab test outside, the development of the hardware setup was frozen as presented in Figure 1.
5. Field pretest: All used hardware was built into the cases, the power supply was installed and the LTE based control network was set up. The Train ATO was emulated by a car; the equipment was mounted on the hood of the car. The Train X was mounted on a tripod as for most tests in railway environment. Static and dynamic tests were performed up to a link distance of 500 m in open field environment.

4.2 Test Scenarios

The test scenarios defined in FP2R2DATO D48.4 Chapter 5.2 reflect 5 major test cases in a railway environment with high number of typical objects along railway tracks. The test cases defined in FP2R2DATO D48.4 Chapter 5.7 reproduce the movement of trains coupling and decoupling, driving in constant distance on the same track or passing each other on parallel tracks. These test cases are typical for VCTS and SDFW in a railway station or shunting yard environment.

The test scenarios presented in Table 1 vary from the proposed field test cases in FP2R2DATO D48.4 Table 3, as the availability of tracks changed one week before the tests. In Figure 7 a satellite image of the NS shunting yard in Amersfoort is shown. The tracks are indicated from A to L, and the positions for starting and stopping or the static positions of communication nodes are indicated. In comparison to the image, the yard was fully parked with trains except for Track A and B. Hence, tests on Track J and tests with trains parked on Track A were not possible. The test scenarios were adapted to driving either on Track B with a clear Track A or driving on Track A with a clear Track B as listed in Table 1.

Due to the given limitations of available tracks and consequently limited possibilities of environments the evaluation of SRC and RL suffers by two potential interesting test cases. Firstly, the trains are driving or one train is approaching next to a platform. Secondly, a large object (parked train) is blocking the SRC signal in a curved track segment.

The environment of a shunting yard or railway station is very complex in case of wireless propagation. The transmitted and directly received signal, so called Line of Sight (LoS) signal, suffers from path loss and shadow fading along the propagation path. In addition, the transmitted signal is reflected or scattered by surrounding objects. These reflected and scattered multipath components (MPCs) experience individual path loss, different Doppler frequency shifts due to relative movement and higher delay due to the larger propagation path than the LoS signal. The LoS signal and all MPCs superimpose at the receiver. Depending on the richness of MPCs and their power relative to the LoS signal, the receiver can process the signal and decode the transmitted data or information is lost. To simulate the SRC and RL behavior in such a railway environment a realistic propagation model considering path loss, shadow fading, delay spread and Doppler frequency spread for the used frequency range and bandwidth would be required. Although the topics are very interesting, unfortunately neither propagation measurements as basis for the modelling, nor the generation of a channel model was part of this project. Hence, convincing simulations of SRC and RL in a railway environment are not possible at this stage.

In addition to the planned test scenarios, two tests for future applications with JCAS in railway applications were conducted. First, the influence on the T2T communication of one or several non-equipped persons parallel to the track or crossing the track was measured while Train ATO was driving back and forth. The investigations could give an indication, if persons or objects on the track can be recognized by the changing propagation conditions of the T2T communication. Second, one person was equipped with a UWB device (c.f. Figure 1: Track worker) walking parallel to tracks and crossing Track B while Train ATO was static on Track B at 50 m. The tests will clarify, if a person equipped with a SRC and RL device (e.g. mobile phone) can be located by equipped trains. The information could be used to either stop the trains in case of a potential collision or for warning the track worker of approaching SDFW or VCTS.

4.3 Test Schedule

The tests were performed within 2.5 days. NS blocked the first two tracks (Track A and B) of the shunting yard, provided the ATO test train SNG 3002 (Train ATO) for 3 days and an additional SNG train (Train X) for one day. All performed tests and the time schedule is listed in Table 2.

The first half day (day 0) was used for installation, static pre-tests and calibration. The Train ATO was parked on Track B.

On the first test day (day 1) and second test day (day 2) test cases described in Table 1 were conducted based on the availability of trains and tracks as listed in Table 2. The second train for dynamic test of Train X was only available on day 1 till 4 pm. Hence, test case 4 and 5 were scheduled for day 1 in the morning and early afternoon.

Test cases 1, 2 and 3 were performed with moving Train ATO and static Train X. The communication node for Train X was mounted on a tripod in front of a buffer stop. Those tests were planned for day 2.

4.4 Safety

The NS Train Test Centre performed a risk assessment based on the scenarios planed in FP2R2DATO D48.4 and discussion together with DLR scientists. The assessment considers three major risks:

- Risk of the test train being damaged by measuring equipment outside of the test train.
- Danger of the test train colliding with a stationary train.
- Danger of test personnel being hit.
- For all risks several actions were set to reduce the occurrence probabilities and the consequences in case of occurrence: Integration and mounting of the test equipment to be checked regularly
- Place static equipment outside of train gauge
- Enlarged safety margin to parked trains (5-10 m)
- All trains are driven by NS test drivers
- Between all train drivers and test leader voice communication is ensured
- Reduced speed during testing
- Crowd controller
- All participants must complete the
    - safety training ("Bevoegd Spoorbetreder"),
    - wear personal protection (safety shoes, yellow reflecting vest),
    - complete the safety briefing and
    - comply with the instructions of NS personnel.

Table 1: Test cases

Test case					Train ATO – Node A				Train X – Node B				Ground – Node C	
#	Name	Manoeuver	Environment	Scenario	Start [m]	Stop [m]	Velocity [km/h]	Track	Start [m]	Stop [m]	Velocity [km/h]	Track	Track	Position [m]
1	VCTS coupling	One train is approaching a static train on same track without actual coupling	Clear A	1.1	350	0	5-10	B	0	0	0	A or B	0-A or B-C	140
			Clear B	1.2	350	0	5-10	A	0	0	0	A or A	0-A or B-C	120
2	VCTS de-coupling	One train is departing a static train on the same track without actual de-coupling	Clear A	2.1	0	350	5-10	B	0	0	0	A or B	0-A or B-C	140
			Clear B	2.2	0	350	5-10	A	0	0	0	A or B	0-A or B-C	120
3	Fixed distance	Static, multi positions	Clear A	3.1	350	0	0-10	B	0	0	0	B	B-C	140
4	Passing	On parallel tracks, one static train, one train is driving back and forth	Clear A	4.1	0	350	5-10	B	60	60	0	A	B-C	140
				4.2	260	0	5-10	B	60	60	0	A		
5	Coupled mode	A platoon is driving back and forth with a fixed distance between the trains.	Clear A	5.1	350	80	5-10	B	260	0	5-10	B	B-C	140
				5.2	80	350	5-10	B	0	260	5-10	B		
6	Sensing	One moving and one static train, non-equipped moving persons	Clear A	6.1	350	0	5-10	B	0	0	0	B	B-C	80
				6.2	0	350	5-10	B	0	0	0	B		
7	Sensing	Two static trains, equipped moving person	Clear A	7.1	100	100	0	B	0	0	0	B	0-A	80

Table 2: Test schedule

Day	Time	ToDo	Case	Name	Maneuver	Equipment	Tracks	Environment
0	13:00	Installation			All static	Train-X Buffer stop, Leica Track B (left) 0 m	Train ATO Track B, Train-X Track B	
	16:00	Static Pre-Tests and Calibration						
	18:00	Remove equipment						
1	8:15	Installation						A parked train was removed from Track A
	10:30	Test	4	Passing	Train ATO driving back and forth	Train-X on 2nd Train	Train ATO Track B, Train-X Track A	Train-X static on Track A
	11:45	Shunting			Drive Train X on Track B, Drive Train ATO on Track B	Change Leica to Track A (right) 60 m		Clear Track A
	12:30	Lunch						
	13:30	VCTS Show Case	5	Coupled mode	Both trains driving back and forth	Train-X on 2nd Train	Train ATO Track B, Train-X Track B	Clear Track A

	14:40	VCTS Test Case	5	Coupled mode	Both trains driving back and forth	Train-X on 2nd Train	Train ATO Track B, Train-X Track B	Clear Track A
		Shunting			2nd Train left	Change Train-X to buffer stop, place Leica Track B (left) 0 m		Clear Track A
	17:00	Sensing	6	Sensing	Train ATO Driving back and forth, non-equipped Track worker moving along and cross Track B	Train-X Buffer stop	Train ATO Track B, Train-X Track B	Clear Track A
	18:30	Remove equipment						
2	8:00	Installation						
	10:00	Test	3	Fixed distance	Train ATO static on multiple points	Train-X Buffer stop	Train ATO Track B, Train-X Track B	Clear Track A
		Test	1+2	VCTS Coupling-Decoupling	Train ATO driving back and forth	Train-X Buffer stop	Train ATO Track B, Train-X Track B	Clear Track A
	11:50	Test	1+2	VCTS Coupling-Decoupling	Train ATO driving back and forth	Train-X Buffer stop, change Ground node	Train ATO Track B, Train-X Track B	Clear Track A

						setting to from Channel 2--2 to Channel 2--5.		
	12:15	Lunch						
	13:00	Test	1+2	VCTS Coupling-Decoupling	Train ATO driving back and forth	Train-X Buffer stop, change Ground node to Track A (left) and setting to Channel 2--2	Train ATO Track B, Train-X Track B	Clear Track A
	14:15	Test	7	Sensing	Train ATO static, equipped Track worker moving along and cross	Train ATO 100 m, Train-X Buffer stop	Train ATO Track B, Train-X Track B, Track worker Track B	Clear Track A
	15:00	Test	1+2	VCTS Coupling-Decoupling	Train ATO driving back and forth	Train-X Buffer stop	Train ATO Track A, Train-X Track B	Clear Track A
	15:30	Test	1+2	VCTS Coupling-Decoupling	Train ATO driving back and forth	Train-X Buffer stop	Train ATO Track A, Train-X Track A	Clear Track B
	15:45	Remove equipment						
	19:30	Closing						

Figure 7: Satellite image of the NS shunting yard Amersfoort with track and position indicators [12]

5 TEST REPORT

The tests reported in this chapter were carried out by qualified test drivers in a controlled environment on a non-public NS shunting yard in Amersfoort/Netherlands.

5.1 Achievements

5.1.1 Test Cases

All planned test cases could be executed. Even though the scenarios had to be adopted due to track occupation, more than 100 runs accumulated for all test cases like VCTS coupling and de-coupling, fixed distance, passing and coupled mode were performed.

To the author's knowledge, two regular trains running in short distance on the same track coupled by a wireless link was performed for the first time. This scenario reflects the VCTS coupled mode and provides highly valuable data for SRC and RL analysis.

5.1.2 VCTS Show Case

In the VCTS show case the SRC+RL test equipment was used to provide radio based real time distance estimation to the train driver for the first time. The distance information was well received by the train drivers and facilitated the manual distance control between the two trains driving on the same track back and forth.

5.1.3 Public relations

The test campaign was documented by a DLR video and photo team. The video material recorded and pictures taken during the tests were used at multiple dissemination channels:

- Documentation video at DLR Institute of Communications and Navigation youtube channel [13]
- Posts at DLR Institute of Communications and Navigation LinkedIn channel
- DLR press release [14]
- DLR Magazine [15]
- DLR internal newspaper "Echtzeit"
- Bahn Manager Magazine [16]

5.2 Collected Test Data

All communication nodes, sensors and ground truth systems recorded data during the two days of testing. As mentioned in Chapter 3.4, the recording of all data sets was synchronized by GNSS based NTP servers. In the following sub-chapters, the different data sets are explained. For each type of data format an example of the stored file with header and exemplary data points is presented. For the analysis presented in Chapter 6, import filters were designed to read the stored files based on the shown structure.

5.2.1 UWB

For the test cases the recorded UWB data is saved in *.txt files in the format as shown exemplarily in Table 3. The table is transposed for easier reading and CIR 2 to CIR 148 are removed. For the evaluation of the reliability of the SRC the fields for PacketIndex, the date and time, and the MessageID were used. For the evaluation of the RL the fields for the date and time, and the fields for MyLastTxTimeStamp, ReceivedTimeStamp and TransmitTimeStamp RepAnchor are processed.

Table 3: Example of UWB data recorded in a *.txt file

PacketIndex	1	2	3	4	5
Year	2025	2025	2025	2025	2025
Month	04	04	04	04	04
Day	29	29	29	29	29
Hour	09	09	09	09	09
Minute	47	47	47	47	47
Seconds	14	14	14	14	14
Microseconds	20279	140118	260117	380123	500148
ReceivedAnchor	2	2	2	2	2
MessageID	182639	182640	182641	182642	182643
MyLastTxTimeStamp	2.7456E+11	2.8222E+11	2.8989E+11	2.9756E+11	3.0523E+11
ReceivedTimeStamp	2.7494E+11	2.8261E+11	2.9028E+11	2.9794E+11	3.0561E+11
TransmitTimeStamp RepAnchor	8.2775E+11	8.3542E+11	8.4309E+11	8.5076E+11	8.5842E+11
firstPathIndex	747.219	747.953	748.797	749.703	750.797
maxPathIndex	749	750	751	752	754
regSlopeIndex	47822	47869	47923	47981	48051
rx_power	-668.016	-67.115	-667.508	-669.986	-672.387
rx_snr	208.323	203.561	212.554	205.786	200.185
rx_fpp	-730.528	-754.066	-748.595	-743.952	-757.129
CIR0	126-98i	1-104i	-106-2i	151+44i	79-104i
CIR1	135-68i	135-68i	135-68i	135-68i	135-68i
⋮	⋮	⋮	⋮	⋮	⋮
CIR149	29+48i	29+48i	29+48i	29+48i	29+48i

5.2.2 GNSS

The GNSS data of all three receivers is stored in the Septentrio's proprietary Sepentrio Binary Format (SBF). Based on the SBF post-processing corrections can be applied and commonly used

GNSS formats like NMEA, RINEX, etc. can be extracted. The recorded SBF GNSS data was processed with a tool called Inertial Explorer Version 9.00.2207 and stored in a *.txt file. As shown in Table 4, the *.txt file contains the GPS time, the position on different coordinate system, the velocity and the position quality. The position accuracy was improved by applying Real-Time Kinematic (RTK) positioning corrections.

Table 4: RTK post-processed GNSS data examples

GPSTime	sec	199870	199870,1	199870,2	199870,3
X-ECEF	m	3904126.73	3904126.73	3904126.72	3904126.72
Y-ECEF	m	366391.78	366391.78	366391.77	366391.78
Z-ECEF	m	5013527.38	5013527.36	5013527.35	5013527.36
Latitude		52 09 22.36040	52 09 22.36011	52 09 22.36008	52 09 22.36002
Longitude		5 21 40.86621	5 21 40.86615	5 21 40.86588	5 21 40.86633
H-Ell	m	52.723	52.707	52.698	52.703
v_{East}	m/s	-0.481	-0.489	0.271	0.227
v_{North}	m/s	-0.408	-0.466	0.355	0.764
v_{Up}	m/s	-1.039	-1.045	1.958	0.599
v_X-ECEF	m/s	-0.269	-0.226	0.892	-0.256
v_Y-ECEF	m/s	-0.508	-0.512	0.356	0.204
v_Z-ECEF	m/s	-1.071	-1.111	1.764	0.942
SDX-ECEF	m	0.132	0.132	0.132	0.132
SD-v_X-ECE	m/s	0.54	0.45	0.422	0.407
SDY-ECEF	m	0.055	0.055	0.055	0.055
SD-v_Y-ECE	m/s	0.416	0.338	0.32	0.311
SDZ-ECEF	m	0.099	0.099	0.099	0.099
SD-v_Z-ECE	m/s	0.756	0.702	0.662	0.63
Q		6	5	5	5

Table 5: Example of Leica tracking data recorded in a *.txt file

LeicaPacket	0	1	2	3	4
Hour	7	7	7	7	7
Minute	47	47	47	47	47
Second	24	24	25	26	26
Millisecond	173	785	466	31	836
LeicaSample	TS_Day2_000061	TS_Day2_000062	TS_Day2_000063	TS_Day2_000064	TS_Day2_000065
PosX	661531.7340	661531.7341	661531.7341	661531.7341	661531.7342
PosY	5781043.0489	5781043.0489	5781043.0486	5781043.0486	5781043.0491
PosZ	517.706	517.706	517.707	517.709	517.704
Date	29.04.2025	29.04.2025	29.04.2025	29.04.2025	29.04.2025
Time	09:45:26.5	09:45:27.1	09:45:27.8	09:45:28.3	09:45:29.1

5.2.3 Leica

The Leica TS was setup in the European Terrestrial Reference System 1989 (ETRS89). Amersfoort is withing the Universal Transverse Mercator (UTM) zone 31. With this information the recorded UTM PosX/PosY/PosZ coordinates can be transferred to World Geodetic System 1984 (WGS84) latitude, longitude and height and plotted on a geo-referenced satellite image. The position tracked by Leica TS in tracking mode was stored on the Leica laptop in *.txt files with the format shown in Table 5.

The static measured positions of fixed objects like the static Train X, the Ground station, the buffer stop, the poles of the overhead line system and the front of the building was stored on the Leica internal storage. The data was stored in Leica proprietary data format and can be exported by the Leica Infinity software to different coordinate systems like UTM East-North-Up (Ost, Nord, Ortho. Höhe) or WGS84 Latitude-Longitude-Height (Breite, Länge, Ellip. Höhe) listed in Table 6. As the Leica TS was set up in German, the data is stored German as well as shown in Table 6. The coordinates in Table 6 are the positions of the poles of the overhead system next to Track A.

Table 6: Example of Leica static data exported to a *.txt file by Leica Infinity software

Punktnr.	pole001	pole002	pole003	pole004	pole005
Punktklasse	Gemessen mit TPS	Gemessen mit TPS	Gemessen mit TPS	Gemessen mit TPS	Gemessen mit TPS
Quelle	R2Dato	R2Dato	R2Dato	R2Dato	R2Dato
Ost [m]	661496.6375	661442.4599	661397.0186	661346.9919	661270.0475
Nord [m]	5781057.95	5781066.475	5781073.68	5781081.554	5781093.25
Ortho. Höhe [m]	50.1219	50.1079	50.087	50.1443	50.1597
KQ 3D [m]	0.005	0.0051	0.0052	0.0054	0.0058
KQ 2D [m]	0.005	0.0051	0.0052	0.0053	0.0056
KQ 1D [m]	0.0002	0.0003	0.0006	0.0009	0.0014
Breite WGS84 [°]	52°09’22.92“N	52°09’23.25“N	52°09‘23.53“N	52°09’23.84“N	52°09‘24.30“N
Länge WGS84 [°]	5°21’39.04“O	5°21‘36.20“O	5°21‘33,83“O	5°21‘31.21“O	5°21’27.18“O
Ellip. Höhe WGS84 [m]	50.1219	50.1079	50.087	50.1443	50.1597
Kartesisch X WGS84 [m]	3904114.898	3904111.837	3904109.221	3904106.435	3904102.432
Kartesisch Y WGS84 [m]	366355.7482	366301.348	366255.7173	366205.4889	366128.2474
Kartesisch Z WGS84 [m]	5013535.851	5013542.149	5013547.458	5013553.33	5013562.049
Datum/Uhrzeit	28.04.2025 15:47	28.04.2025 15:48	28.04.2025 15:49	28.04.2025 15:50	28.04.2025 15:52

5.2.4 LiDAR and Magnetic Field Sensors

The LiDAR and magnetic field sensor data is stored together in Robot Operating System

(ROS) bags based on a ROS2 implementation. The LiDAR point cloud was extracted for each time stamp into the format shown in Table 7. A standard LiDAR viewer tool can read this format and show either the static point cloud of one time stamp or show a sequence of multiple time stamps as a video.

Table 7: LiDAR point cloud data for one time stamp

messageType	'sensor_msgs/PointCloud2'
header	1x1 struct
height	1824
width	16
fields	6x1 struct
is_bigendian	0
point_step	22
row_step	352
data	642048x1 uint8
is_dense	0

The magnetic field data was not used for the SRC and RL analysis, and therefore is out of scope.

5.3 Lessons Learned

These tests involved several teams at NS and DLR. The number of staff involved increased up to 35 to the time of testing. The execution of railway tests demands long term preparation with different tasks and staff demands:

- 2.5 years: Initial interaction between NS and DLR and explanation of intentions.
- 2 years: First test equipment design. Iterative process for technology development with purchasing of parts, lab tests and redesign.
- 1 year: Detailed description of test goals, potential equipment and estimated effort exchanged.
- 10 months: First working meeting between DLR and NS and on sight inspection. Kick-off for detailed planning.
- 4 months: First outdoor pre-tests.
- 3 months: Week 18 2025 for tests fixed. Core test team consolidated.
- 1 month: Final test schedule and plan. Risk assessment and safety measures by NS.
- 3 weeks: Final outdoor pre-tests individual systems.

- 2 weeks: Final GO for tests. Participants on sight fixed; hotel, transport and catering organized.
- 1 weeks: Final outdoor pre-tests full setup.
- 2 days: Packing and transport to test sight.
- 1 day: Installation and start testing.

The remote control was established on 3GPP LTE public network. The servers hosting the VPN were located in Munich/Germany. We experienced the following issues with this network setup:

- The coverage of the public cellular network is hard to predict and changing locally.
- The preparation of the tests and the tests itself were performed in different countries. Hence, contractual issues in case of data limitations occurred with a German mobile data contract in the Netherlands.
- Conventual contracts may offer unsymmetric conditions for up and down link. Symmetric communication conditions would be preferred.
- Due to the large distance between the hosting servers at DLR in Munich/Germany and the tests in Amersfoort/Netherlands, increased latency had to be considered.

More effort needs to be invested in video documentation. The focus of the video team was to document the work performed by the participants, partially filming the test scenarios but not test equipment. For post processing, a video documentation of all scenarios, covering all nodes of the test architecture and most of the surrounding would be beneficial. The video material should be synchronized to the measurement equipment and the video frames time stamped. Such a system could be seen as an additional ground truth system.

6 ANALYSIS

The analysis of the test data will show the communication error of the SRC and the distance error of the RL. The analysis is provided for the most prominent test cases one to four. Test case five was used for demonstration purpose and test cases six and seven are out of scope for this analysis. The necessary data handling is described as well.

6.1 TEST DATA HANDLING AND COMBINATION

The collected data was split in two data sets: the communication data set, and the reference time and position data set.

All time stamps in all data sets were transformed to the time zone Central European Summer Time (CEST) for an easy alignment and filtering.

6.1.1 UWB Communication Data Set

The recorded data exchange between the UWB communication nodes is used to derive the SRC and RL performance of the used communication system. The timespan of the data set useful for SRC and RL performance analysis were marked, cut out and aligned with the timing and position reference data set. The UWB communication data set contains two independent data sets from two subsystems, one using omni-directional antennas and one using directional antennas. In the following analysis, the results of the subsystem with the omni-directional antennas are indicated in red, the results of the subsystem with the directional antennas are indicated in blue as shown in Figure 8.

6.1.2 Time and Position Reference Data Set

The Leica, Lidar and GNSS data is used as reference data for all analysis with respect to the recording time, and with respect to the time varying position of each unit and the resulting time varying distance between the units for the RL analysis. Furthermore, the time varying position is used to plot the absolute position of each node on a geo-referenced satellite image for visualization. Therefore, all positions are stored in Cartesian XYZ coordinates and WGS84 latitude, longitude and altitude coordinates. The omni-directional UWB antennas, the directional UWB antennas, the GNSS antennas, the LiDAR and the Leica prism were on different locations in x and z direction on the boxes as shown in Figure 8. In y direction, all devices were aligned and mounted in the middle of the box. The offset in x and z direction is compensated in the analysis.

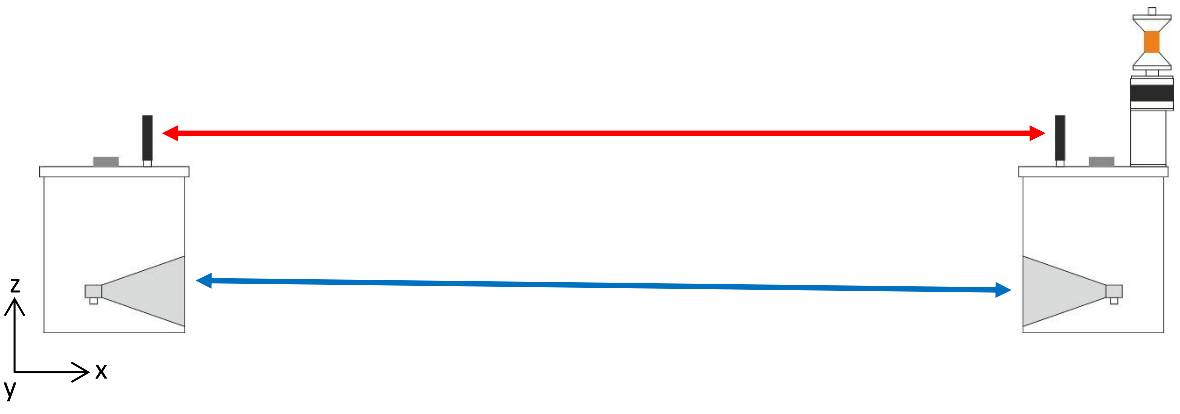

Figure 8: Drawing of the antenna and prism position

6.2 SRC PERFORMANCE

The communication performance is evaluated based on the occurrence of consecutive packet errors and the total packet error rate (PER).

6.2.1 Consecutive Packet Errors

For safety critical applications, like the distance control of two trains driving in short distance, the age of information needs to be small. This can be achieved with a high update rate at the transmitter and a low occurrence of consecutive packet errors at the receiver. As the update rate is limited for each communication device, the analysis of the occurrence of consecutive packet errors is very important.

Examples of multiple runs forth and back from 250 m to roughly 3 m and back to 250 m are shown in the top chart of Figure 9 and Figure 11. The occurrence of consecutive packet errors is plotted in relation in the bottom chart. The measurements for test case one, two and four were performed dynamically, whereas for test case 3 shown in Figure 10, the tests were performed static every 10 m up to 250 m.

In Figure 9 it can be clearly seen, that the sub-system based on omni-directional antennas experiences larger numbers of consecutive errors when the distance is increased. The sub-system based on directional antennas is hardly experiencing consecutive packet errors. These findings are even more visible in the representation of the consecutive packet errors over distance in Figure 12. For this chart, 28 runs forth and back between 250 m and 3 m were used. For omni-directional antennas indicated in red, it can be observed that within 0 to 80 m, sparse events with 2 to 5 consecutive packet errors occur. Up to a distance of 200 m, consecutive errors of maximum 12 missing packets occur. For distances up to 250 m, the consecutive errors increase with maximum rates 20 missing packets. For the directional antennas indicated in blue, the number is not exceeding two consecutive packet errors from 3 to 250 m. Zero consecutive packet errors indicate a transmission without packet errors.

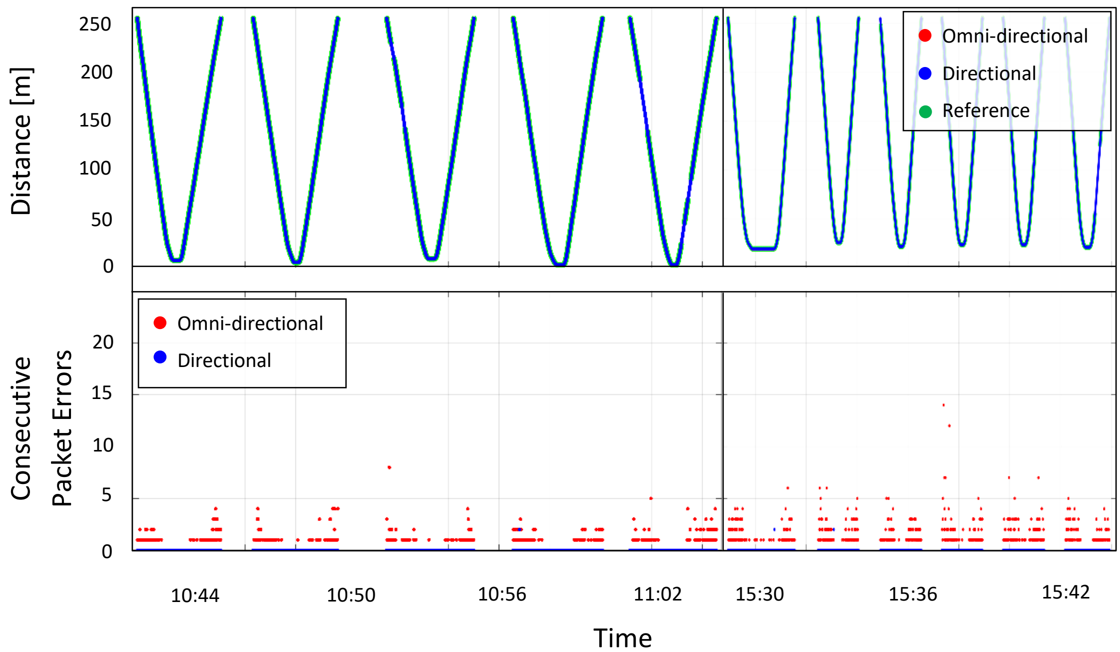

Figure 9: Distance and consecutive packet errors for 11 runs of test case 1+2

For the static tests shown in Figure 10 the results show a similar behaviour of an increased number of consecutive errors for larger distances. At three positions (187 m, 216m and 225 m) the system based on directional antennas experience an increased number of errors in comparison to the dynamic tests shown in Figure 9. As the propagation conditions are very dependent on the geometry of the environment, static positions can result in constructive or destructive communication behaviour and strongly varying communication errors for different communication ranges. This behaviour is even better represented by the results shown in Figure 14.

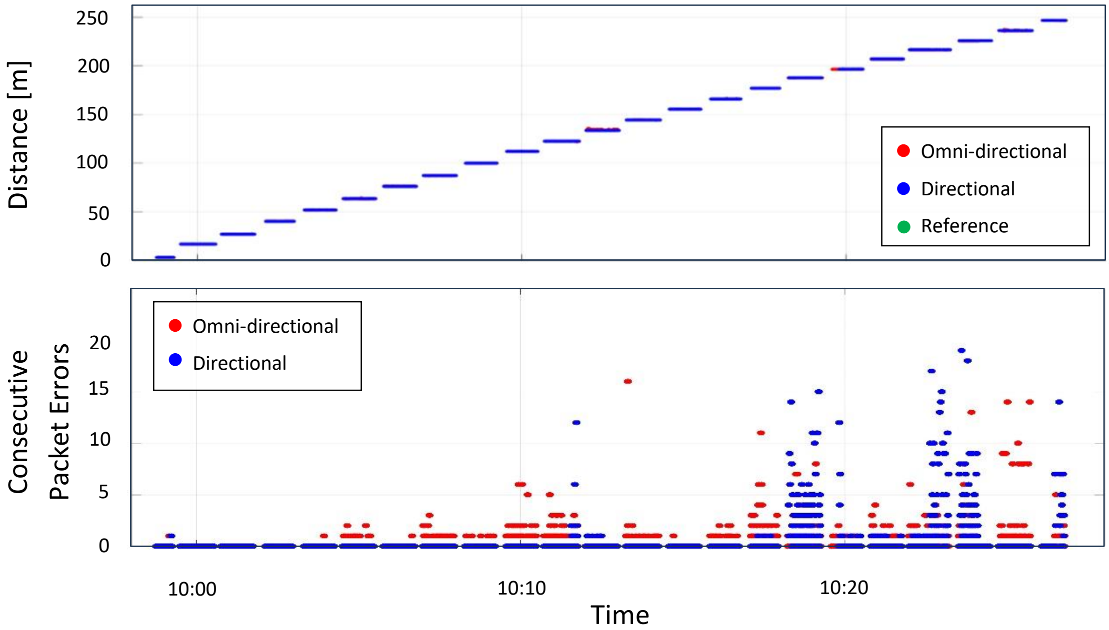

Figure 10: Distance and consecutive packet errors for static tests (test case 3)

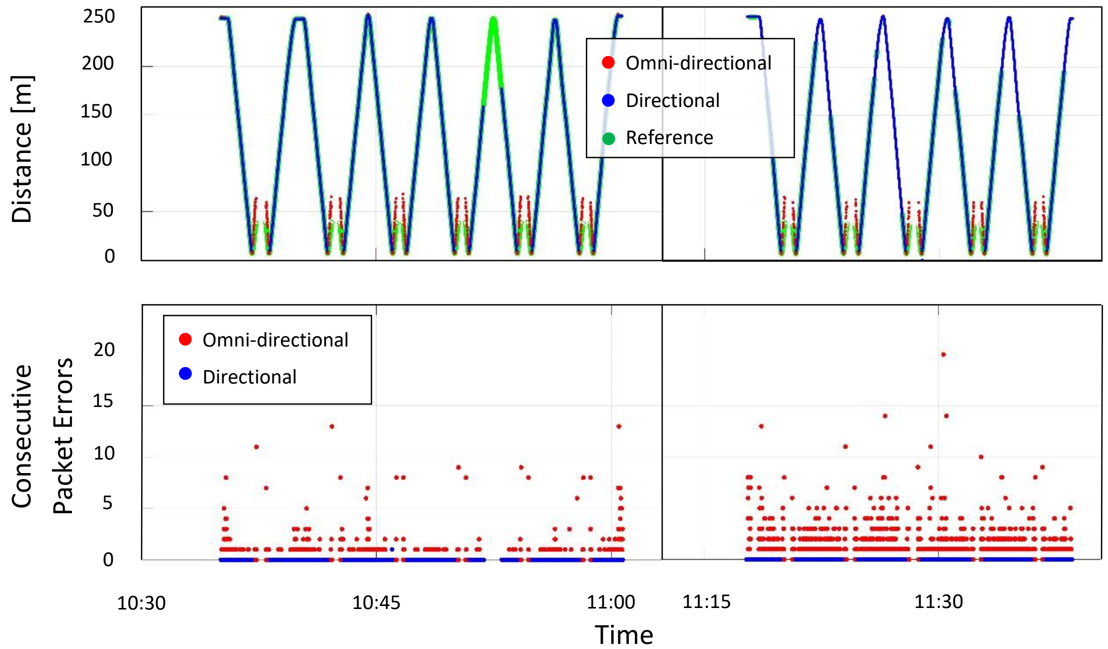

Figure 11: Distance and consecutive packet errors for 11 runs of test case 4

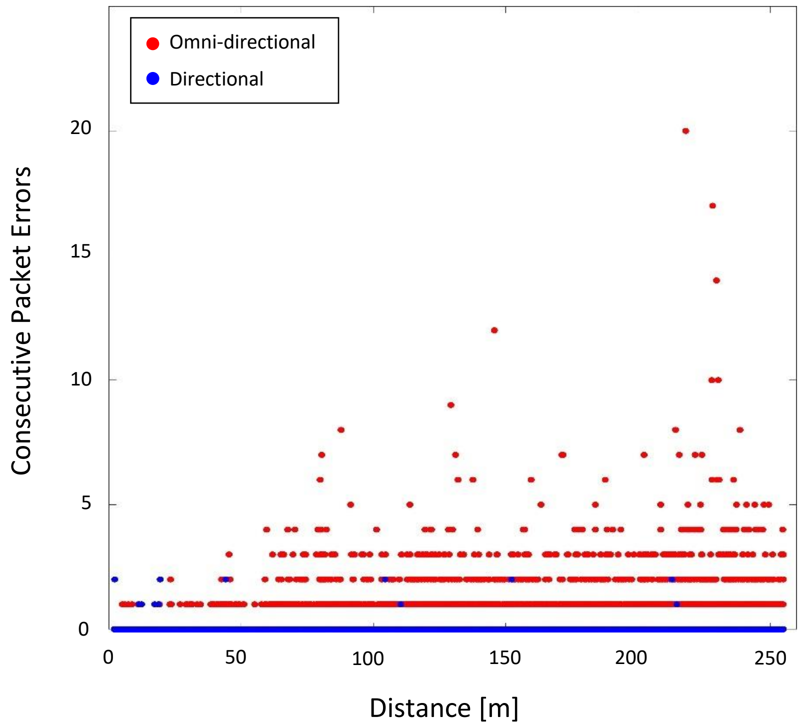

Figure 12: Consecutive packet errors over distance of all runs of test case 1+2

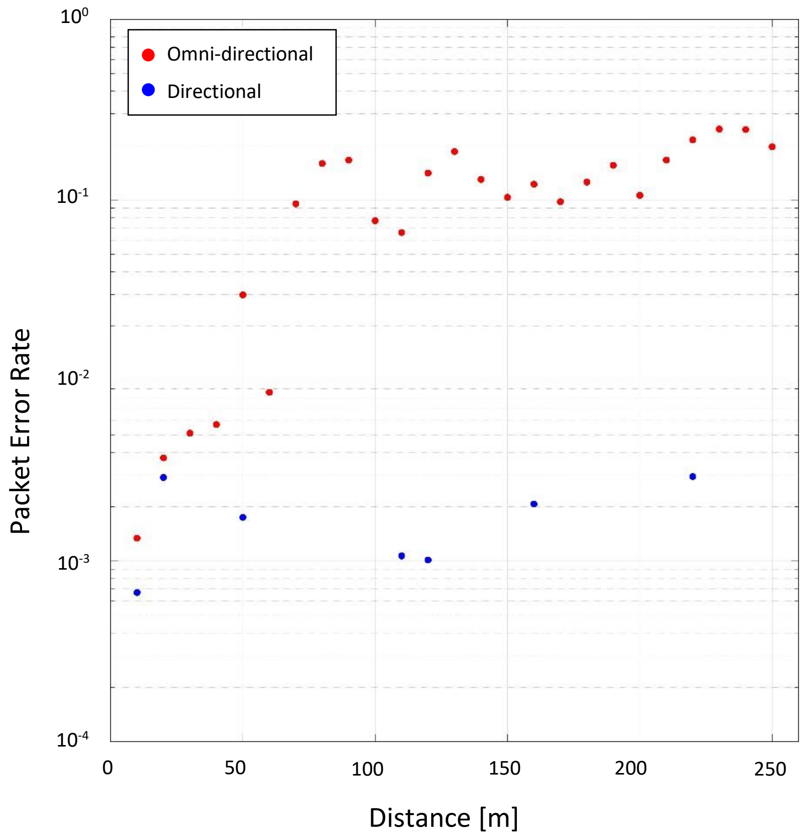

Figure 13: Packet error rate over distance of all runs of test case 1+2

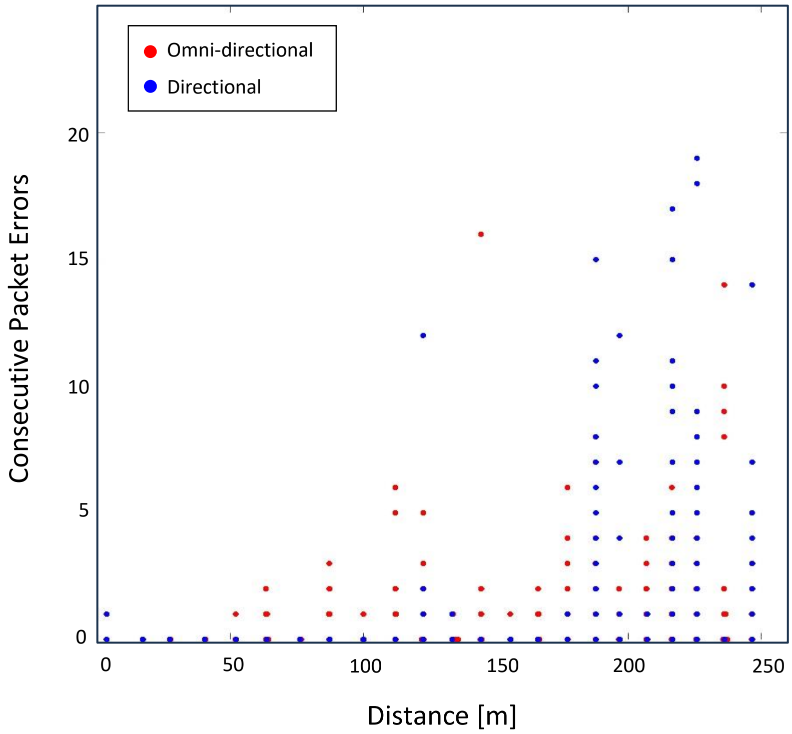

Figure 14: Consecutive packet errors over distance of all runs of test case 3

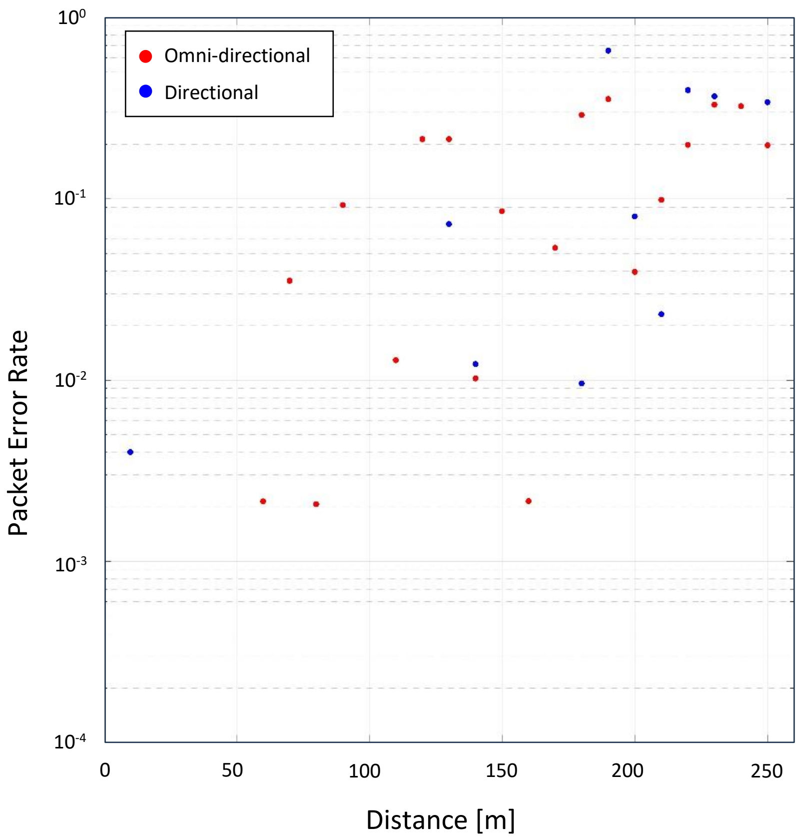

Figure 15: Packet error rate over distance of all runs of test case 3

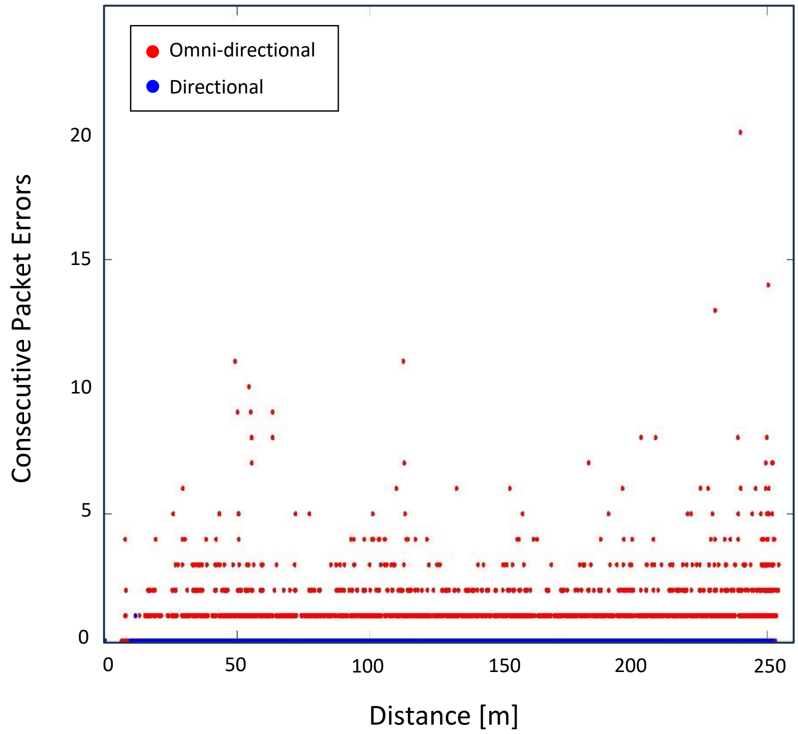

Figure 16: Consecutive packet errors over distance of all runs of test case 4

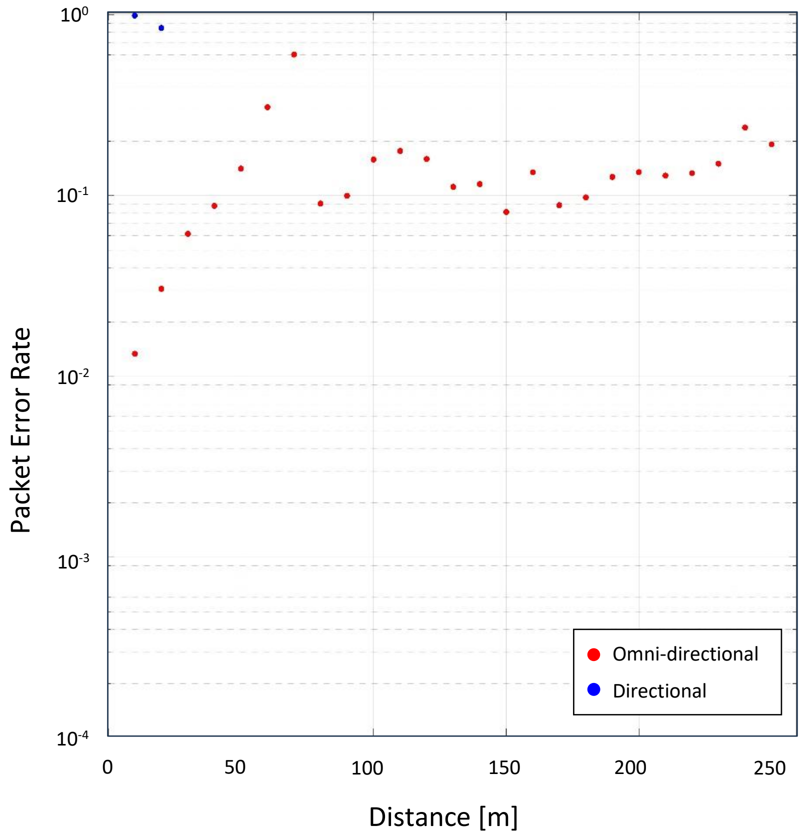

Figure 17: Packet error rate over distance of all runs of test case 4

Test case 4 represents a train passing a second standing train on a parallel platform (c.f. Figure 19). In the LoS condition we observe similar results for the consecutive packet error as for test case 1 and 2. In the case of an obstruction of the signal by the train bodies (non-LoS condition) the system based on the omni-directional antennas can receive reflected signal components for the first 35 m. From 35 to 70 m packets are received very sparsely, which results in a high number of consecutive errors for these distances. The system based on the directional antennas is not able to receive those reflected signal components and the connection is interrupted from the time, both communication nodes are on the same position along track. In both cases, before the communication stops, the errors increase tremendously in the non-LoS condition as shown in Figure 16.

6.2.2 Packet Error Rate

The most common measure for a communication system is the PER over the signal to noise ratio (SNR). The PER can be also depicted over distance. The distance is indirect proportional to the SNR. This means with increasing distance the received power is decreasing, and with it, the SNR is decreasing. In Figure 13, Figure 15 and Figure 17 the PER is shown in relation to the distance for the sub-systems with omni-directional antennas in red and with directional antennas in blue. The shown dots are the accumulated PER within distance intervals of 10 m of all runs of each test case.

For test case 1 and 2 represented by Figure 13, the PER for the omni-directional antennas is increasing with increasing distance from around 10^{-3} at 10 m to 10^{-1}up to 80 m. From 80 to 250 m, the PER fluctuates between 10^{-1} and $2 \cdot 10^{-1}$. The high PER at distances above 80 m can be explained by the railway environment. The metallic objects like parked trains, overhead line masts and fences cause MPCs. The omni-directional antenna at the receiver collects all these MPCs which may cause inter symbol interference which results in unusable packet information. For the directional antennas, the PER starts at $7 \cdot 10^{-4}$ and fluctuates between 10^{-3} and $3 \cdot 10^{-3}$ from 20 to 250 m. The high PER at short distances of 10 m can be explained by the saturation of the receiver due to the high antenna gain of the directional antennas. Several distance intervals (e.g. 30, 40, 60, 70, … m) are not represented by blue dots, as the PER was zero. In comparison to the omni-directional antenna, the directional antenna is only collecting a small fraction of the caused MPCs in the direction of the main lobe of the antenna. These results to a tremendous decrease of the PER.

As mentioned before, the static tests results in a strong variation of packet errors for different distances. As well as for the omni-directional, but also for the directional based system the PER varies between 10^{-3} and $5 \cdot 10^{-1}$ as shown in Figure 15.

The PER results for test case 4 strongly relate to test case 1 and 2 for LoS conditions. In the non-LoS condition, the behaviour of the consecutive packet errors are reflected also in the PER chart in Figure 17. The red dots between 35 and 70 m increase the PER of test case 1 and 2 as well as the blue dots at 10 and 20 m.

6.2.3 SRC Performance Conclusion

For both subsystems, with the omni-directional and the directional antennas, we need to state the following limitations of the analysis:

- The test track was too short to test the limits of the communication system. Especially for the directional antennas, the system could have been tested for way longer distances, in an environment with shadowed line of sight (LoS) signal or the transmit power could have been reduced to experience significant PER at the limit of the communication system.

- The collected test data should be extended with simulations to generate a multiple times larger data set as it is now with around $7 \cdot 10^4$ packets. For PER evaluations in order of 10^{-6} the data set would need to encompass 10^7 to 10^8 data packets transmitted.

The overall test performance of the UWB based system for T2T SRC is very promising. The number of consecutive errors is low even for large distances and the PER can be limited with the use of directional antennas. The data exchange within the SRC specifications can be ensured even within the strongly influencing railway propagation environment. For the most prominent test case (1+2) the PERs for all distance intervals and sub-systems are listed in Table 8.

Advancements could be achieved by a more sophisticated active power control to prevent the receiver from saturation. The use of antenna arrays with beam steering capabilities would reduce the inter symbol interference in a similar way as the directional antennas, with the advantage of better reception in curved track segments. The general position of the antenna in the front area could be optimized dependent on the train body and used antenna type.

6.3 RL Performance

The RL algorithm outputs the distance between two communication nodes. As the nodes were installed both at the coupler of the trains, or one on the coupler and one on a tripod emulating a parked train as shown in **Fehler! Verweisquelle konnte nicht gefunden werden.** and Figure 19, the distance between the nodes correspond to the distance between the train fronts facing each other.

Figure 18: Indicated LoS signal of the SRC and RL measurement links with omni-directional antennas (red line) and directional antennas (blue line) on the same track (test case 1, 2, 3)

(a) LoS conditions (b) non-LoS conditions

Figure 19: Passing maneuver of two trains on parallel tracks (test case 4)

6.3.1 Estimated Distance and Distance Error

The distance between the trains is estimated with the double-sided round trip time (DS-RTT) algorithm based on multiple time measurements between the UWB communication nodes. The detailed algorithm is explained in the deliverable FP2R2DATO D48.4.

The distance error is the error of the UWB DS-RTT results in comparison to the estimated distance of a ground truth system. A Leica TS was used as ground truth system to measure the position of fixed communication nodes before each test and to track the moving communication node mounted on the train during the test. Based on this data set, the distance between the communication nodes on the trains could be estimated independently from the UWB test system.

It needs to be stated that, the accuracy of the ground truth is also limited and the measurements can be influenced by the environment. If the accuracy of the test system is in the same order of magnitude as the ground truth system, the resulting distance error is a combination of both systems and a clear allocation of the error is not possible. Within the tests, we observed several misalignments of the Leica TS measurements. Within the postprocessing of the Leica TS data, multiple outliers and a stronger variation than expected of the position tracking were observed. To a certain extend the outliers could be compensated, but in combination with the unexpected variations the accuracy exceeded the expected limits of 2 cm specially when the tracked train was moving or reflections of the sun on the train body around the prism were disturbing the Leica TS.

The estimated distance of the two UWB sub-systems and the Leica reference (indicated in green) for 11 test runs of test case 1 and 2 on April 29th is shown in the top chart of Figure 20. As the distance estimation of the sub-system with the omni-directional antenna and the sub-system with the directional antenna are very close, the blue dots indicating the directional antenna are overlapping the red dots of the omni-directional data. The resulting distance error is plotted below for all runs. A variation of the distance error between ±1 m can be observed. For a more detailed analysis Figure 21 shows only one run between 10:51 and 10:55 in the morning. It can be clearly seen, that the variations increase with the distance between the trains and that the distance error strongly fluctuates when the train is moving. In the time from 10:53.15 to 10:53.50 the train is static. Around 10:52, the Leica TS lost track two times which results in the gap of the distance error analysis.

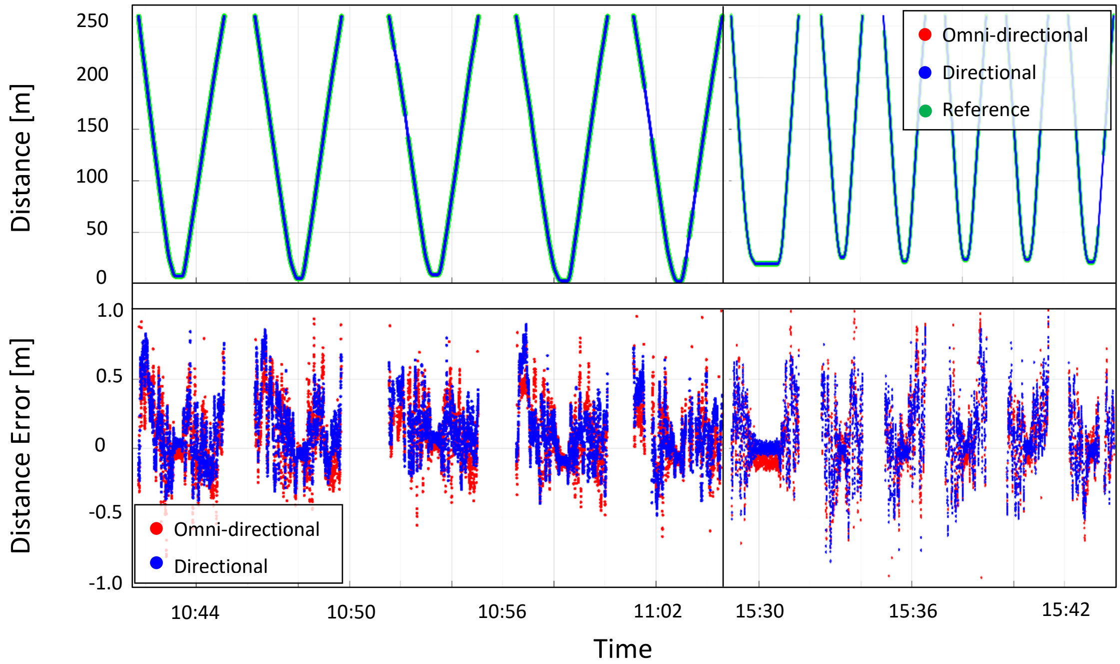

Figure 20: Distance and distance error over time for 11 runs of test case 1+2

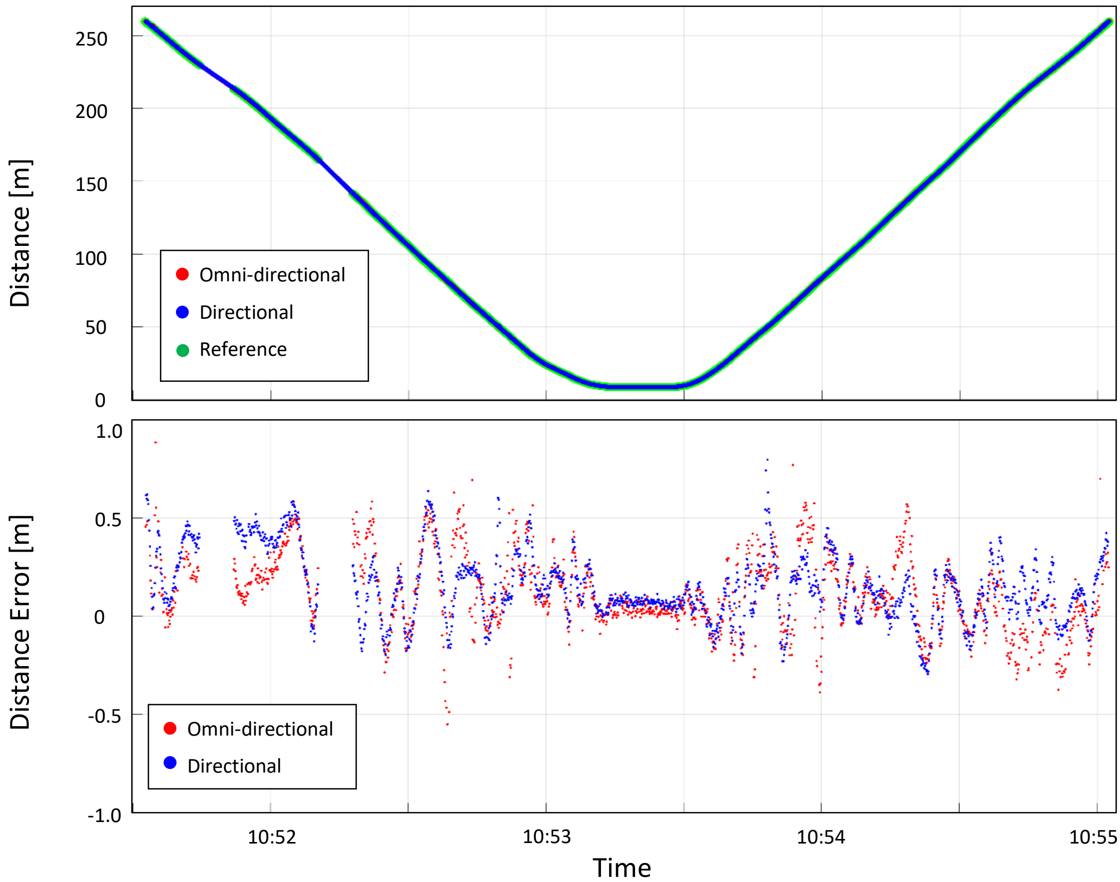

Figure 21: Distance and distance error over time of one run of test case 1+2

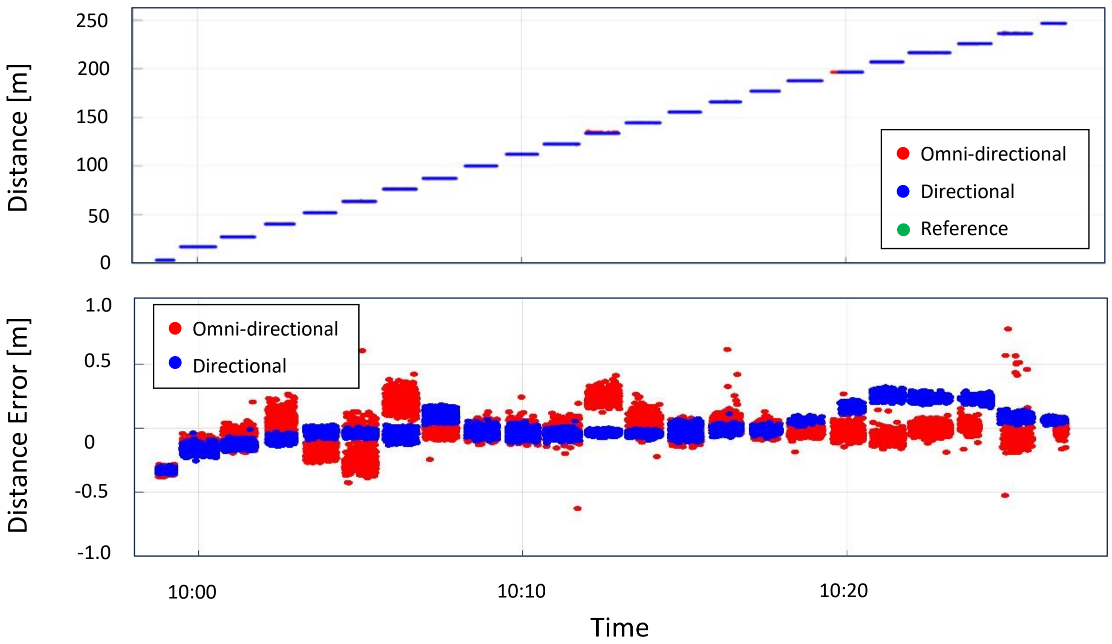

Figure 22: Distance and distance error over time for static tests (test case 3)

The static tests show the potential of RL in railway environments in Figure 22. Except from minor and very sparse outliers, the distance error is within ±40 cm for omni-directional and ±30 cm for directional antennas up to a link distance of 250 m.

Similar to the the SRC behaviour, the analysis of the RL accuracy for test case 4 needs to be split in LoS condition and non-LoS condition. In Figure 23 we see for all 11 runs the good alignment between the reference (indicated in green) and the UWB DS-RTT results from 250 m down to 6.5 m and 10 m representing the omni-directional system in red and the directional system in blue, respectively. At 10 m distance the parallel offset of the tracks is too large for the opening angle of the directional antennas and the connection get lost. At 6.5 m the communication nodes mounted on the train fronts are next to each other and we transit from the LoS condition to the non-LoS condition. Whereas the UWB DS-RTT results for the directional system is abruptly stopped only with an increase of the distance error, the system based on the omni-directional antennas receives reflected signals. Those signals experience a larger propagation delay which results in an increased RL distance error till to the point, where the communication is lost. This behavior is shown in detail in Figure 24.

To analyse the behaviour of the UWB based DS-RTT distance estimation on different distances between the trains, the distance error is plotted against the distance in Figure 25, Figure 26 and Figure 27. In those figures the left plot (a) shows the distance error over distance and the right plot (b) shows the distribution of the accumulated distance error. For test case 1 and 2 it can be observed, that the distance error is only slightly increasing from ±20 cm at 3 m to ±60 cm at 50 m and to ±80 cm at 250 m with very sparce outliers not exceeding ±1 m. The distribution chart shows a strong concentration between ± 60 cm in Figure 25.

In Figure 26 representing the static tests of test case 3 we see even more prominent the small distance error even for high distances and a very strong concentration between ± 30 cm and ± 20 cm for the omni-directional and the directional antenna system, respectively. The ± 20 cm distance error reflects the lower bound based on the used communication bandwidth of the UWB system.

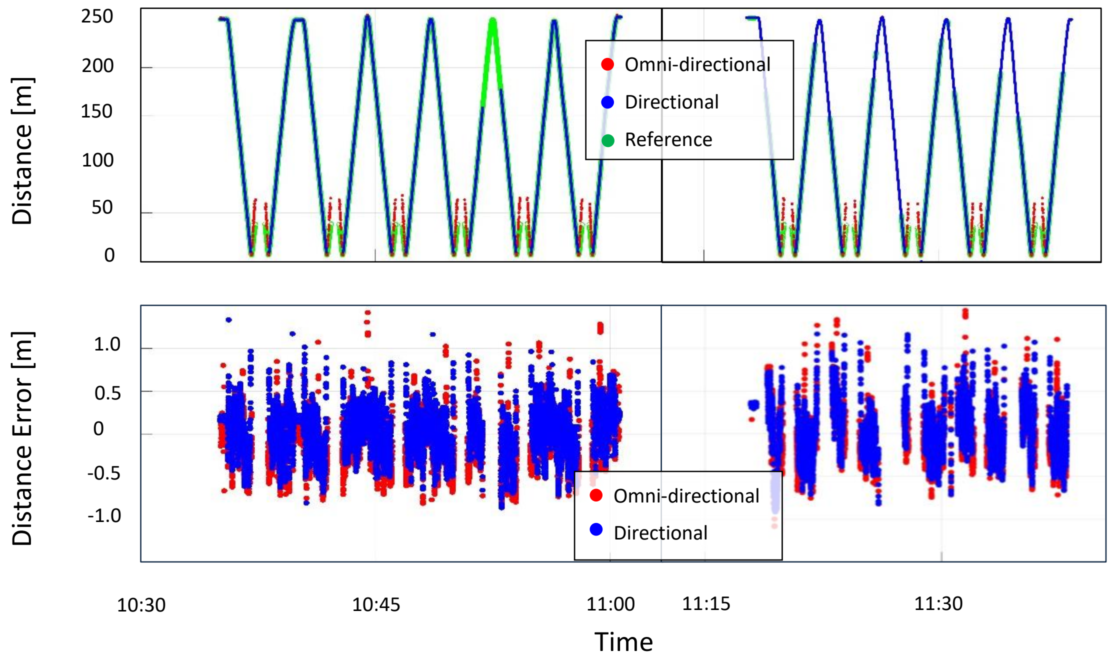

Figure 23: Distance and distance error over time for 11 runs of test case 4

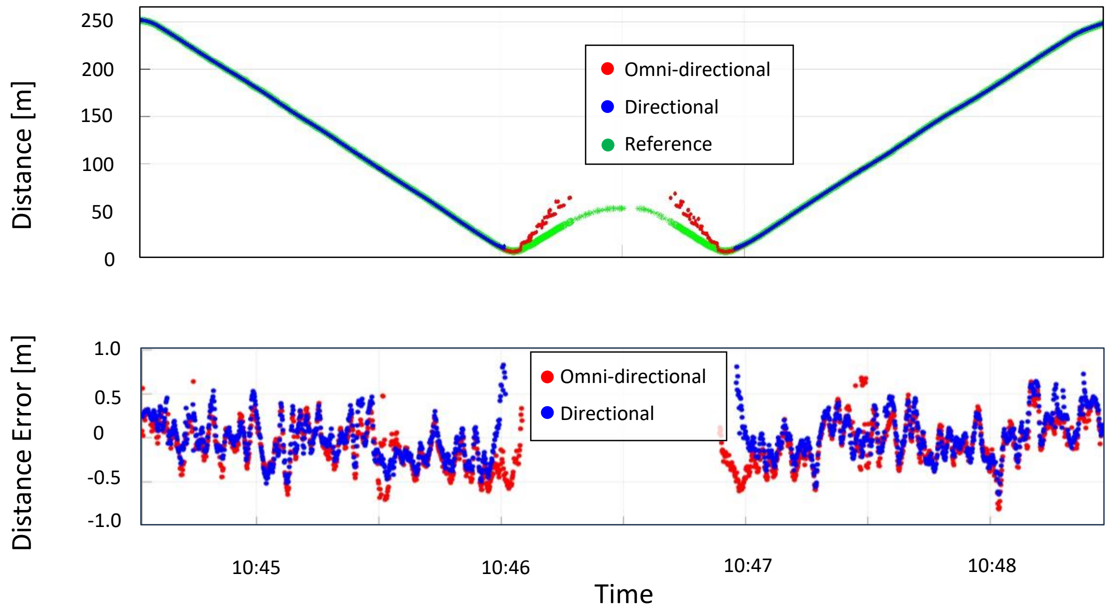

Figure 24: Distance and distance error of one run of test case 4

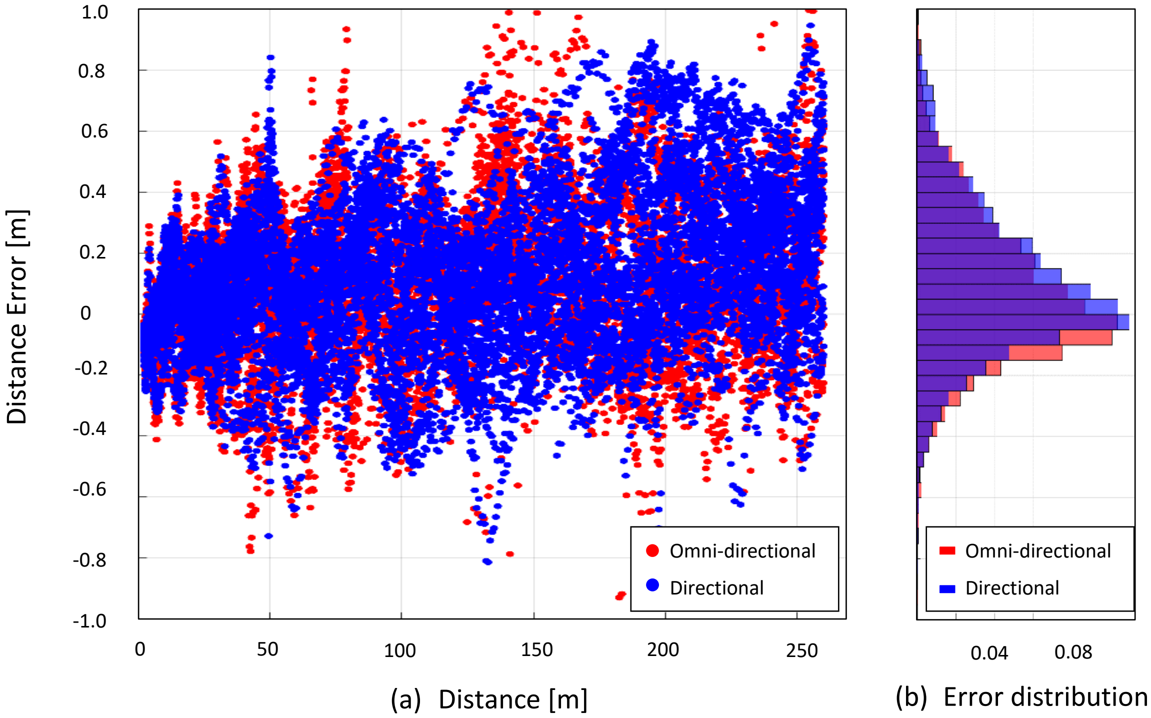

Figure 25: Distance error over distance and error distribution of test case 1+2

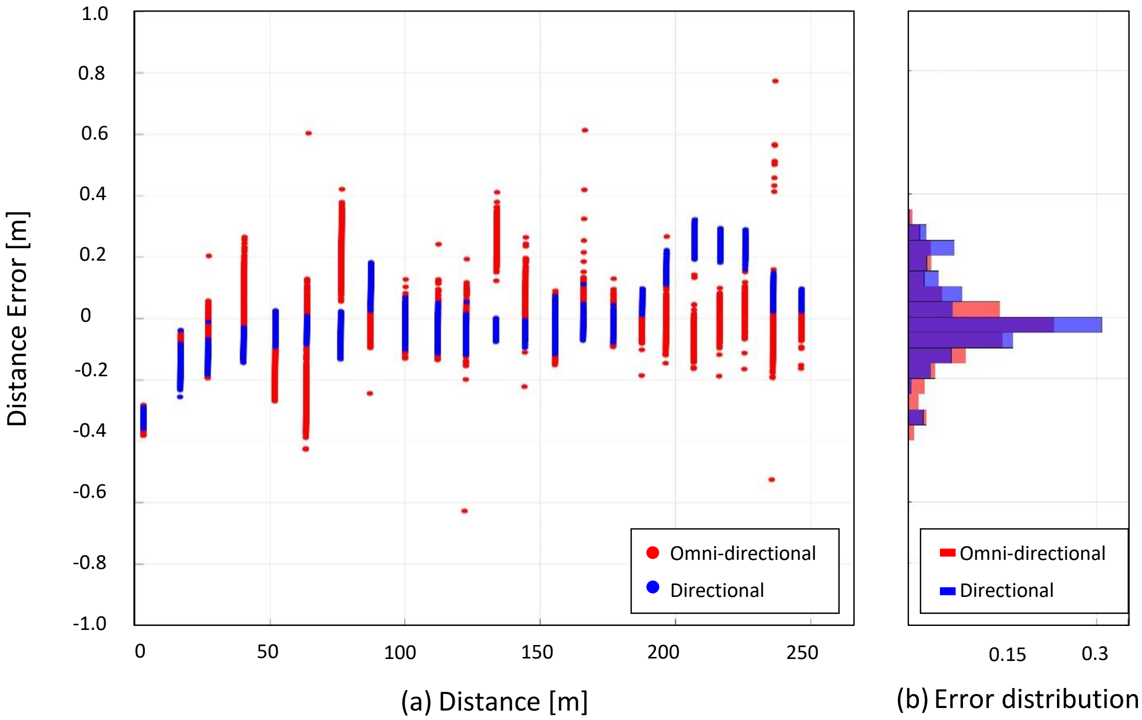

Figure 26: Distance error over distance and error distribution of test case 3

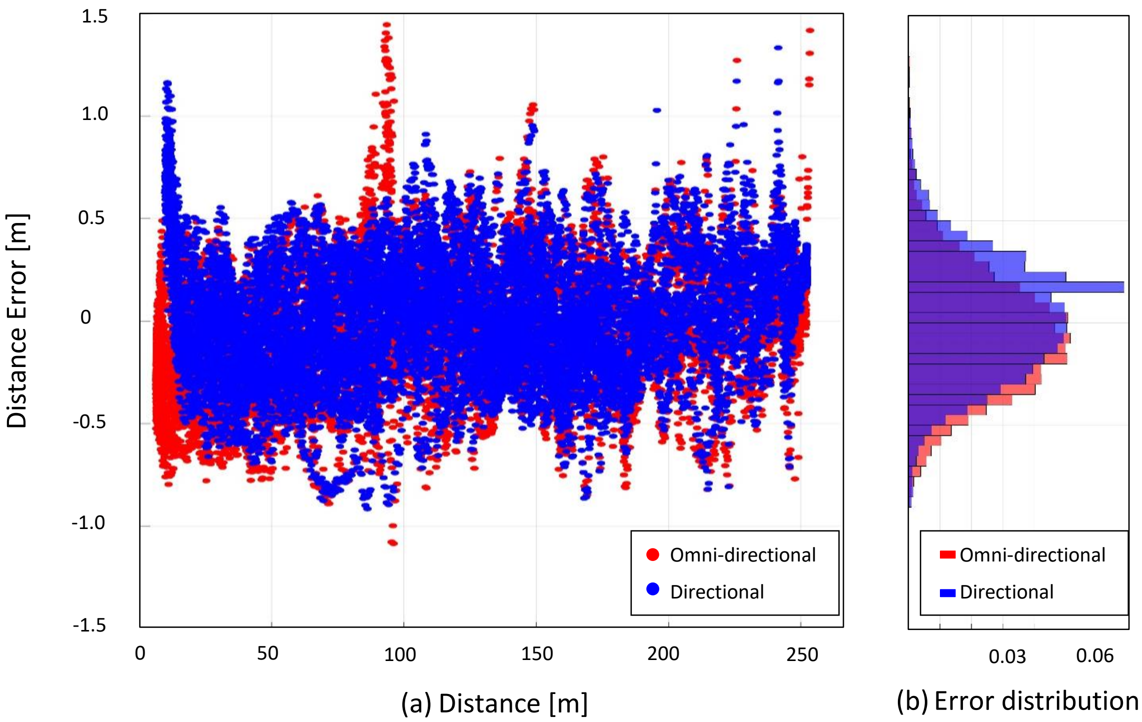

Figure 27: Distance error over distance and error distribution of test case 4

The distance error over distance for test case 4 is shown in Figure 27 (a). For large distances, the distance error is comparable to the one for test case 1 and 2. The behaviour of an increased distance error in the phase of communication loss at 10 m (blue indicated directional system) and in case of non-LoS condition starting at 6.5 m can be clearly seen. In addition, the increased distance error for the omni-directional system at 80 to 90 m need to be mentioned. This error occurs in multiple runs and results from the propagation conditions and geometry at this distance. As these outliers only occur for the omni-directional antenna system, it is assumed that the affecting MPCs are caused by a strong reflection by fence to the left of track A only visible for omni-directional antennas. The concentration of the distance error between ± 80 cm is slightly broader as for test case 1 and 2. For the directional antenna based system the loss of communication can be clearly seen with an increased error concentration at 20 cm in Figure 27 (b).

6.3.2 RL Performance Conclusion

With both sub-systems, a distance estimation could be provided within the whole range of 250 m. The RL test performance analysis showed an accuracy between ±20 cm to ±80 cm dependent on the distance between the trains. The lower bound of ±20 cm is set by the used bandwidth and the limitations of the hardware implementation of the UWB system. Similar accuracy was achieved with the same system in indoor scenarios.

The differences in accuracy between the two sub-systems based on omni-directional antennas and directional antennas are neglectable. Across the different test cases a distance error within the same order of magnitude dependent on the communication distance could be found. Nevertheless, the geometry of the environment can influence the RL system as well as the occurrence of non-LoS conditions. The statistical details for intervals with a distance span of 10 m are listed in Table 8 for test case 1 and 2. The accumulated distance error for each distance span was fitted with a gaussian distribution and the resulting mean error, the standard deviation, as well as the root mean square error (RMSE) are listed. This numbers can be used to simulate the movement control of trains driving in a certain distance behind each other.

The strong variation up to ±1 m is a product of the influence of the railway environment on the UWB transmission and the inaccuracy of the ground truth reference system. Furthermore, the influence of movement can not be assigned to the UWB system. Hence, an investigation on different velocities with a different ground truth system would be beneficial. Overall, improvements could be shown with a more stable, accurate and reliable ground truth system. Furthermore, the achievable accuracy with different bandwidths would be of interest to transfer the gained knowledge to other communication systems with different communication bandwidths.

Table 8: SRC and RL statistics for test case 1+2

Distances	Omni-Directional				Directional			
	Packet Error Rate	Distance Mean Error	Distance Standard Deviation	Distance RMSE	Packet Error Rate	Distance Mean Error	Distance Standard Deviation	Distance RMSE
[m]		[m]	[m]	[m]		[m]	[m]	[m]
0-10	0.00134	-0.0424	0.0836	0.0937	0.00067	-0.0271	0.0902	0.0942
10-20	0.00373	-0.0259	0.1265	0.1291	0.00290	0.0251	0.1061	0.1089
20-30	0.00511	-0.0008	0.1225	0.1225	0	0.0072	0.1013	0.1015
30-40	0.00571	0.0300	0.1899	0.1921	0	0.0539	0.1653	0.1737
40-50	0.02981	0.0584	0.2787	0.2845	0.00175	0.1016	0.2355	0.2563
50-60	0.00860	0.0269	0.1881	0.1899	0	0.0451	0.2237	0.2280
60-70	0.09510	-0.0030	0.2435	0.2435	0	0.0107	0.1949	0.1950
70-80	0.15921	0.2208	0.2785	0.3551	0	0.0859	0.2048	0.2219
80-90	0.16624	0.0224	0.2233	0.2241	0	0.2010	0.1763	0.2672
90-100	0.07668	0.0760	0.2566	0.2673	0	0.0781	0.2815	0.2918
100-110	0.06592	0.0555	0.2409	0.2469	0.00107	0.0185	0.2527	0.2531
110-120	0.14079	0.0885	0.1899	0.2092	0.00101	0.0737	0.1987	0.2117
120-130	0.18544	0.0965	0.2771	0.2930	0	0.0165	0.2258	0.2261
130-140	0.12981	0.3210	0.2616	0.4138	0	0.0334	0.2551	0.2570
140-150	0.10334	0.2533	0.2965	0.3896	0	0.0788	0.2321	0.2448
150-160	0.12208	0.2130	0.2600	0.3357	0.00207	0.1581	0.2331	0.2814
160-170	0.09769	0.1703	0.2608	0.3111	0	0.1134	0.2408	0.2659
170-180	0.12551	0.1133	0.3237	0.3425	0	0.1390	0.2616	0.2960
180-190	0.15546	0.1151	0.3089	0.3292	0	0.1944	0.3111	0.3665
190-200	0.10601	0.1072	0.3279	0.3446	0	0.2459	0.3311	0.4122
200-210	0.16632	0.1074	0.2553	0.2766	0	0.2832	0.2732	0.3933
210-220	0.21519	0.1190	0.2494	0.2760	0.00294	0.2793	0.2579	0.3800
220-230	0.24670	0.1165	0.2409	0.2672	0	0.2584	0.2541	0.3622
230-240	0.24544	0.1095	0.2206	0.2460	0	0.2150	0.2249	0.3109
240-250	0.19692	0.1371	0.2685	0.3011	0	0.1827	0.2366	0.2988

7 CONCLUSIONS

The results presented in this deliverable provide critical and actionable insights into the feasibility and performance of Short-Range Communication (SRC) and Relative Localization (RL) as foundational technologies for enabling innovative operational solutions such as Virtually Coupled Train Sets (VCTS) and Self-Driving Freight Wagons (SDFW). The comprehensive testing campaign, supported by real-world test cases, feedback from train drivers and project partners, and in-depth analysis of empirical data, unequivocally demonstrates the technical potential and operational relevance of these technologies in rail environments.

The tests were conducted in a representative and complex railway environment: the NS shunting yard in Amersfoort, Netherlands, which features a catenary overhead line system, multiple parallel tracks, parked trains, and surrounding infrastructure such as buildings and fence. This setting closely mirrors real-world operational conditions, making it a highly relevant and challenging testbed for evaluating the robustness and reliability of T2T communication and localization systems under realistic interference and dynamic conditions.

The test system developed by the DLR was based on IEEE 802.15.4 Ultra-Wideband (UWB) chipsets, leveraging the high time-resolution and large bandwidth inherent to UWB technology. Two distinct antenna configurations (omni-directional and directional) were evaluated in parallel to assess their impact on performance. The analysis revealed that directional antennas significantly improved link quality, reducing interference and enhancing signal stability due to their focused radiation patterns. However, even with omni-directional antennas, reliable data exchange was consistently achieved over distances up to 250 m, which corresponds to the expected operational range for VCTS and SDFW. This confirms that the selected SRC technology is not only capable of supporting safety-critical functions but also resilient enough to operate under practical constraints.

The RL results demonstrate a distance estimation accuracy within ±20 cm to ±80 cm across the full tested operational range. While this accuracy is influenced by the large bandwidth of the UWB system and environmental factors such as multipath propagation and signal blockage, it represents a level of precision that is exceptionally difficult to achieve with alternative technologies, especially in dense, obstructed environments like shunting yards or other typical railway environments. This order of magnitude of accuracy is particularly significant for gap supervision, dynamic spacing control, and collision avoidance in VCTS, where maintaining safe and stable vehicle distances is paramount.

In summary, the test outcomes confirm that the T2T-based SRC and RL system is capable of delivering a highly available data exchange and a decimeter accurate distance estimation required for the safe and stable operation of VCTS and SDFW. The ability to enable decentralized, real-time coordination between rail vehicles without reliance on fixed infrastructure marks a transformative step toward fully autonomous rail operations.

The integration of SRC and RL into the onboard architecture of VCTS enhances system resilience, supports advanced coupling and supervision concepts, and enables a more flexible, scalable, and efficient use of rail capacity. Furthermore, by decentralizing control and safety functions, these technologies lay the groundwork for a new paradigm in train operation; one where individual vehicles can act as intelligent agents assisted by Autonomous Route Setting (AnRS).

While this deliverable establishes a strong technical foundation, further research is required to fully understand the impact of SRC and RL on intra-platoon dynamics, control stability, and system-level safety under varying operational conditions. Future projects should focus on closed-loop control validation, failure mode analysis, certification pathways, and the integration of SRC and RL into a unified decentralized wireless communication system serving different communication needs in railways.

In conclusion, the successful testing of SRC and RL in a representative railway environment represents a significant step forward in the development of innovative operational solutions and autonomous rail systems. The results not only validate the technical feasibility of the chosen approach but also provide a solid, evidence-based foundation for advancing innovation in high-automation rail operations.

REFERENCES

[1] G. West, “Taoglas Omni-Antenna TU.60.3H31.” Taoglas, Jan. 16, 2023. Accessed: Nov. 13, 2024. [Online]. Available: https://www.taoglas.com/datasheets/TU.60.3H31.pdf

[2] Yeung Yu Kai and Conroy Jack, “Taoglas Horn-Antenna PHA.01.A.” Taoglas, May 28, 2019. [Online]. Available: https://www.taoglas.com/datasheets/PHA.01.A.pdf

[3] Partron, “Dielectric Chip Antenna Datasheet.” Partron, Jan. 15, 2018. [Online]. Available: https://download.datasheets.com/pdfs2/2021/11/19/15/36/33/59284/prtrn_/manual/partron-acs5200hfauwb_c224424.pdf

[4] B. Siebler, O. Heirich, and S. Sand, “Train Localization with Particle Filter and Magnetic Field Measurements,” in *2018 21st International Conference on Information Fusion (FUSION)*, Cambridge, United Kingdom: IEEE, Jul. 2018, pp. 1–5. doi: 10.23919/ICIF.2018.8455298.

[5] B. Siebler, A. Lehner, S. Sand, and U. D. Hanebeck, “Snapshot Estimator for Magnetic Field-Based Train Localization with Uncalibrated Magnetometers,” in *2025 33rd European Signal Processing Conference (EUSIPCO)*, Palermo, Italy: IEEE, Sep. 2025, pp. 2142–2146. doi: 10.23919/EUSIPCO63237.2025.11226624.

[6] B. Siebler, O. Heirich, and S. Sand, “Relative train localization with magnetic field measurements,” in *2018 IEEE/ION Position, Location and Navigation Symposium (PLANS)*, Monterey, CA: IEEE, Apr. 2018, pp. 1228–1233. doi: 10.1109/PLANS.2018.8373509.

[7] B. Siebler, O. Heirich, S. Sand, and U. D. Hanebeck, “Joint Train Localization and Track Identification based on Earth Magnetic Field Distortions,” in *2020 IEEE/ION Position, Location and Navigation Symposium (PLANS)*, Portland, OR, USA: IEEE, Apr. 2020, pp. 941–948. doi: 10.1109/PLANS46316.2020.9110149.

[8] O. Heirich, A. Lehner, P. Robertson, and T. Strang, “Measurement and analysis of train motion and railway track characteristics with inertial sensors,” in *2011 14th International IEEE Conference on Intelligent Transportation Systems (ITSC)*, Washington, DC, USA: IEEE, Oct. 2011, pp. 1995–2000. doi: 10.1109/ITSC.2011.6082908.

[9] O. Garcia Crespillo, O. Heirich, and A. Lehner, “Bayesian GNSS/IMU tight integration for precise railway navigation on track map,” in *2014 IEEE/ION Position, Location and Navigation Symposium - PLANS 2014*, Monterey, CA: IEEE, May 2014, pp. 999–1007. doi: 10.1109/PLANS.2014.6851465.

[10] B. Siebler, O. Heirich, and S. Sand, “Bounding INS Positioning Errors with Magnetic-Field-Signatures in Railway Environments,” presented at the 30th International Technical Meeting of The Satellite Division of the Institute of Navigation (ION GNSS+ 2017), Portland, Oregon, Nov. 2017, pp. 3224–3230. doi: 10.33012/2017.15311.

[11] J. D. Hol, F. Dijkstra, H. Luinge, and T. B. Schon, “Tightly coupled UWB/IMU pose estimation,” in *2009 IEEE International Conference on Ultra-Wideband*, Vancouver, BC, Canada: IEEE, Sep. 2009, pp. 688–692. doi: 10.1109/ICUWB.2009.5288724.

[12] Google, “Geo-referenced satellite image.” 2025. [Online]. Available: earth.google.com

[13] DLR Institut für Kommunikation und Navigation, *FP2-R2DATO - Rail to Digital automated up to Autonomous Train Operation - Test Campaign Amersfoort*, (Aug. 08, 2025). [Online Video]. Available: https://www.youtube.com/watch?v=T424LpuiC9U

[14] Denise Nüssle, “DLR testet System für virtuelles Kuppeln in der Praxis,” Aug. 2025, [Online]. Available: https://www.dlr.de/de/aktuelles/nachrichten/2025/dlr-testet-system-fuer-virtuelles-kuppeln-in-der-praxis

[15] Paul Unterhuber, “Folge mir unauffällig,” *DLR Magazin*, Nov. 2025. [Online]. Available: https://www.dlr.de/de/medien/publikationen/magazine/alle-magazine-webversion/dlrmagazin-178

[16] Paul Unterhuber, “Der Schlüssel zur Bahn der Zukunft: Lokalisierung und drahtlose Kommunikation,” *bahn manager*, Dec. 16, 2025. [Online]. Available: https://www.eurailpress.de/abo/bahn-manager.html